NTNU – Trondheim
Norwegian University of
Science and Technology

Clump-weight trawl gear interaction with submarine pipelines

Ingrid Berg Johnsen

Marine Technology
Submission date: December 2012
Supervisor: Svein Sævik, IMT
Co-supervisor: Hagbart Alsos, Reinertsen

Norwegian University of Science and Technology
Department of Marine Technology

NTNU Trondheim
Norges teknisk-naturvitenskapelige universitet
Institutt for marin teknikk

THESIS WORK SUMMER/FALL 2012

for

Stud. tech. Ingrid B. Johnsen

Clump-weight trawl gear interaction with submarine pipelines

Samvirke mellom klumpvekt trålutstyr og offshore rørledninger

A large network of subsea pipelines have been installed at the Norwegian continental shelf and for large diameter cases (> 16") these are in most cases left exposed on the seabed. The fishing activity in the area is often based on bottom trawl gear, consisting of a trawl net kept open by trawl doors, one at each side of the net. The trawl doors are further pulled by a cable connected to the vessel, the purpose of the doors being to keep the cables separated and the trawl net open. In order to allow for two trawl nets, clump weights connected to a separate pull cable may be applied in the middle. The clump weight mass, including hydrodynamic mass may be more than 10000 kg and when its hits a pipeline, two load effects govern:

1. An initial impact that may damage the coating and cause steel wall denting.
2. A "Pull-over" force which is a more long periodic force needed to pull trawl gear such as clump weights and trawl boards over the pipeline. This force depending on the several parameters such as the mass, pipe diameter, free span height and length, cable stiffness, soil stiffness etc.

In many cases, item 2 above governs the design with respect to external loads on subsea pipelines, specially for high temperature pipelines.

This master work focus on the pipeline free-span response due to "Pull-over" loads from clump weights and eventual differences between the results obtained from simulating the physical contact behaviour using SIMLA. The work is to include:

1) Literature study, including trawling technology, offshore pipeline technology including design loads, failure modes and design criteria, recommended practices for pipeline trawl gear loads and response analysis, non-linear finite element methods with focus on the methods applied in the computer program SIMLA and the thesis work already carried out by M.Sc. Martin Møller, Vegard Longva and Kristian Maalø.

2) Establish analysis scenarios with respect to free-span length and height, pipe diameter and mass, warp line length, clump weight design and soil properties including which parameters to be varied. This is to be carried out in cooperation with REINERTSEN.

3) Establish associated SIMLA models and perform analyses for the following scenarios:
   a) Clump weight and warp line model with contact elements using the model established by K. Maalø as a starting point.

b) Compare numerical results with pull-over test data performed by MARINTEK and STATOIL (similar to that performed by K. Maalø)
c) Compare detailed trawl analyses with loads extracted from of point load histories from DNV-RP-F111

4) Discussion of pipeline response quantities and the effect of introducing sensitivity on elements such as: contact friction, altered clump weight geometry, altered center of gravity of clump weight etc..

5) Conclusions and recommendations for further work

The work scope may prove to be larger than initially anticipated. Subject to approval from the supervisors, topics may be deleted from the list above or reduced in extent.

In the thesis the candidate shall present his personal contribution to the resolution of problems within the scope of the thesis work

Theories and conclusions should be based on mathematical derivations and/or logic reasoning identifying the various steps in the deduction.

The candidate should utilise the existing possibilities for obtaining relevant literature.

Thesis format
The thesis should be organised in a rational manner to give a clear exposition of results, assessments, and conclusions. The text should be brief and to the point, with a clear language. Telegraphic language should be avoided.

The thesis shall contain the following elements: A text defining the scope, preface, list of contents, summary, main body of thesis, conclusions with recommendations for further work, list of symbols and acronyms, references and (optional) appendices. All figures, tables and equations shall be numerated.

The supervisors may require that the candidate, in an early stage of the work, presents a written plan for the completion of the work.

The original contribution of the candidate and material taken from other sources shall be clearly defined. Work from other sources shall be properly referenced using an acknowledged referencing system.

The report shall be submitted in three copies:
- Signed by the candidate
- The text defining the scope included
- In bound volume(s)
- Drawings and/or computer prints which cannot be bound should be organised in a separate folder.

Ownership
NTNU and Reinertsen AS have equal ownership of the thesis. Any use of the thesis has to be approved by NTNU or Reinertsen AS.

The department has the right to use the thesis as if the work was carried out by a NTNU employee, if nothing else has been agreed in advance.

Thesis supervisors
Prof. Svein Sævik
Dr. ing. Hagbart Alsos, REINERTSEN

Deadline: 15th December, 2012

Trondheim, Juni 28, 2012

Svein Sævik

Candidate signature:

Preface

This report is a result of my master thesis, compulsory for graduating students in master of science, department of Marine Technology, Norwegian University of Science and Technology. The master thesis is completed in one semester during autumn 2012, and count as 30 credits according to the credit system at NTNU. The master thesis is based on a pre project performed by me during autumn, 2011, dealing with the same subject.

The master thesis is written in collaboration with Reinertsen AS. My supervisors are Prof. Svein Sævik at department of Marine Technology, NTNU, and Dr. ing. Hagbart Alsos at Reinertsen AS. In addition, Kristian Maalø, former employee at Reinertsen AS has been acting as a co-supervisor, especially in assisting with questions regarding SIMLA and input file modelling alterations.

Some alterations to the master description are performed with approval from my supervisors. The alterations are minor, but include changes in which parameters to be altered during sensitivity studies.

I would like to thank Prof. Svein Sævik for excellent guidance during this master thesis. I would also like to thank Hagbart Alsos and Kristian Maalø for help and guidance with the modelled input files, and for great support, feedback and involvement with the master thesis. In addition, I would like to thank Reinertsen AS and Statoil ASA for making model test videos, and making the results from model tests available for verification purposes.

Abstract

Clump weights come in several shapes, with a mass generally between 2 to 9 tons [5]. With extensive offshore development in the last decades, vast networks of pipelines are installed on the sea bottom. With both pipeline extension and trawl equipment development in mind, the need for designing pipelines able to resist forces from trawl gear interaction have emerged. A recommended practice for pipeline design, DNV-RP-F111, was established by DNV. In this master thesis, a brief introduction to trawl gear and recommended practices are given.

The main objective of the master thesis is to reproduce model tests numerically and analyse the response from clump weight over-trawling pipelines. Evidence is sought to establish and differentiate between the importance of various parameters, e.g free span height, pipeline diameter, and pipe end conditions. A number of sensitivity studies were performed, with alterations in several parameters, e.g warp line angle alteration and clump weight wobbling. A full scale pipeline model was also analysed, investigating effects of flexibility in pipelines and comparing the results with design loads.

All analyses are performed in SIMLA, a special purpose non-linear finite element program. A general description of non-linear finite element method is included in the report. All input values used to model the different cases are presented in the master thesis.

A good correspondence linking model test results and reproduced simulated models were generally achieved, with some deviations. The deviations are primarily found for low free spans, indicating that this discrepancy can be reduced by further development of the numerical model, e.g by introducing friction to the model.

For the full scale pipeline model, design loads are evidently higher than

the pull over force from the corresponding full scale simulation. When comparing design loads with pull over forces from simulated experimental test models, they are more closely related. For small diameter pipelines, full scale model simulations with regular pipeline stiffnesses reduce the pull over forces significantly compared to rigid pipeline model simulations. The findings indicate that design load calculations might be too rigid when regarding small diameter full scale pipelines.

Sensitivity simulations indicate a connection between free span height, pipeline diameter and pull over force. For high free spans, the simulated pull over force increase with decreasing pipe diameter. For low free spans, the simulated pull over force decrease when decreasing the pipe diameter.

Clump weight wobbling have in the master thesis been shown to reduce the pull over force. This is seen in the sensitivity analyses performed.

Changing clump weight geometry can lead to significant changes in results. An alteration of the warp line bracket was performed, extending the bracket with 4 cm. The effect was an reduction in the pull over force by approximately 10%, in all cases. A change in warp line angle was also performed, by increasing and then decreasing the angle with 20%. The effect was an reduction in pull over force by 10% and an increase in pull over force by approximately 10%, respectively.

For further details regarding the results, see chapter 5.

Sammendrag

Klumpvekter kommer i ulike former og størrelser, og er normalt mellom 2-9 tonn. Et utstrakt rørledningsnettverk er lagt på havbunnen som en følge av en omfattende offshorevirksomhet og utvikling de siste tiår. På grunn av fare for sammenstøt mellom trålutstyr og rørledninger, ble det utviklet en veiledende fremgangsmåte for rørlesningsdesign i forbindelse med tråd-rør sammenstøt. Denne fremgangsmåten ble designet av DNV, og er forkortet DNV-RP-F111. Både rør, trålmetoder, trålutstyr, og DNV-RP-F111 er omhandlet i masteroppgaven, med et spesifikt fokus på klumpvektsinteraksjon med rør.

Hovedformålet med masteroppgaven er å reprodusere modelltester numerisk, for å finne klumpvektrørledningrespons. Effekten av å endre ulike paramtere i modellen er også beskrevet. De viktigste parameterne som ble endret er rørdiameter, frispennhøyde, grensebetingelser for rør (fleksibelt/fastholdt), i tillegg til flere mindre parameterendringer.

Alle analysene ble analysert i SIMLA, et analyseprogram som benytter ikke-lineær elementmetode. En generell introduksjon til elementmetoden og hvilke metoder som benyttes i SIMLA er inkludert i masteroppgaven. Det er også inkludert et kapittel som viser input-verdier for de ulike delene i datamodellen.

Modelltestresultat og reprodusert simulert resultat hadde generellt god overenstemmelse, med enkelte avvik. Avvikene er hovedsakelig for lavere frispenn, og siden avviket er så konsekvent indikerer dette at avviket i resultat kan reduseres ved videre utvikling av simulert modell. Et forslag kan være å introdusere friksjon, da det ikke lyktes å introdusere dette i masteroppgaven.

For fullskalamodellen er design-lasten, beregnet fra DNV-RP-F111 klart høyere enn de korresponderende fullskala lastene. Når design-laster

sammenliknes med simulerte modelltester samsvarer kreftene i større grad. For rør med liten diameter, vil en fullskala modell redusere pull over-kreftene betydelig.

En klar sammenheng mellom frispennhøyde, rørdiameter og pull over kraft er tydelig når man ser på resultat fra sensitivitetsanalyser. For høye frispenn øker den simulerte pull over-kraften med minkende rørdiameter. For lave frispenn øker pull over kraften med økende rørdiameter.

Klumpvektsanalyser der clumpvekten oscillerer før og under interaksjon er simulert. En økt klumpvekts-oscillering ga en reduksjon i pull over-kraften.

Endring i klumpvektsgeometri kan få følger for pull over-kraften. I masteroppgaven ble warpelinebeslaget forlenget med 4 cm, som resulterte i en reduksjon av pull over-kraft med 10% for alle analyser. En endring i warpelinevinkel ble også utført. Vinkelen ble økt og redusert med 20%, og førte til en henholdsvis minking og øking i pull over-kraft med 10%.

For flere detaljer rundt resultatene, se kapittel 5.

Contents

List of Figures

List of Tables

List of symbols

$\mathbf{\Delta\hat{R}}$	Effective load vector
$\mathbf{\hat{K}}$	Effective stiffness matrix
$\mathbf{C}$	Damping matrix
$\mathbf{K_T}$	Tangential stiffness matrix
$\mathbf{M}$	Mass matrix
$\mathbf{r}$	Displacements in finite element equations
$\mathbf{R^E}$	External force vector
$\mathbf{R^I}$	Internal force vector
$\mathbf{R_{ext}}$	External load vector
$\mathbf{R_{int}}$	Internal force vector
$\mathbf{\ddot{u}}$	Acceleration field
Δt	Time step
δ_p	Global displacement of pipeline at point of clump weight pull-over
ϵ_D	Tolerance level parameter in convergence criteria
γ, β, α	Integration parameters
κ	Strain hardening parameter in yield criterion
$\sigma_\mathbf{0}$	Initial stress tensor
σ	Stress tensor of Cauchy stress
$\mathbf{f}$	Volume force vector
$\mathbf{t}$	Surface traction

$\mathbf{u}$	Displacement vector
ν	Poisson's ratio
ϕ	Warp angle
ψ	Vertical sweep angle
ρ	Material density
θ	Sweep angle, clump weight configuration
θ	Torsion rotation of the neutral axis, in kinematic compatibility
ε	Strain tensor of natural strain
ε^e	Elastic strain
ε^p	Plastic strain
C	Damping coefficient
$C_{a,fs}$	Added mass coefficient, pipeline in free span
$C_{a,sb}$	Added mass coefficient, pipeline at seabed
C_a	Added mass coefficient
C_d	Drag coefficient
c_s	Pipe end damping
d	Water depth
D_r	Roller diameter, clump weight
D_s	Pipe steel diameter
E	Young's modulus (modulus of elasticity)
E_{xx}	Green strain
EA	Axial stiffness
EI	Bending stiffness
F_p	Horizontal pull over force
F_s	Pipe end pretension
F_z	Vertical pull over force
G	Shear modulus

g	gravity
$h^{'}$	Dimensionless moment arm to calculate clump weight pull over load
H_{sp}	Span height (gap between pipeline and seabed)
k_c	Normal contact stiffness
k_s	Pipe end stiffness
k_w	Warp line stiffness
L	Length pipeline
L_{clump}	Distance from clump weight interaction point with pipeline to centre of gravity of clump weight
l_{fs}	Free span length
l_{lw}	Length lower warp
l_r	Roller length
l_s	Length sweep lines
l_{uw}	Length upper warp
m_a	Added mass
m_d	Dry mass
m_s	Submerged mass
m_t	Steel mass
OD	Outer diameter
t_c	Coating thickness
t_h	Pipe steel thickness
T_p	Pull over time
u	Displacement in x direction
V	Trawling velocity
v	Displacement in y direction
w	Displacement in z direction

Chapter 1

Introduction

In Norway, trawling has developed into a large industry with larger and altered trawl gear to increase the trawling efficiency [9]. Larger fishing vessels have been introduced with larger equipment, and the double trawl has increased in scope. A double trawl is held in place by a clump weight, normally weighing between 2-9 tons, placed between the two trawl nets and dragged along the sea bed. Concurrently, Norway has developed an extensive network of offshore pipelines at the sea bed, associated with the offshore oil and gas industry. As fishing equipment is dragged along the sea floor, one could risk trawl gear interference with pipelines. As a consequence, a need for pipeline design able to resist the impact load was brought into attention.

Several studies have been performed on general trawl gear pipeline interactions. Among them, a model test ordered by Statoil, performed at MARINTEK in 1990, focusing on otter doors overtrawling pipelines in free spans [16]. During these tests, a trend where pipelines experience relatively high loads and deflections when otter doors are towed over pipelines was established. Until 2004, no tests on clump weight pipeline interactions were performed [16].

In planning of pipeline installations during the development of the Kristin and Snøhvit offshore oil and gas fields, a need for more data on particularly clump weight pipeline interactions became apparent. Seeing as pipelines would be laid out partly on an uneven seabed, and exposed to trawling activities. A model test investigating clump weight pipeline interactions were performed at MARINTEK in 2004. This model test is in many ways a

basis of the master thesis, where the main objective is clump weight pipeline interactions, also in comparison with model test results.

Chapter 2

Background

2.1 Pipelines

On the Norwegian shelf, over 8600 km of export pipelines are installed transporting product from the oil and gas site to the receiver at shore [1]. As the offshore production site can be far off shore, often very long pipelines are needed to reach the site. They come in several sizes, depending on the carrying capacity they are designed for. The sea bed around off shore production sites are also laid with pipelines, e.g flow lines transporting oil and gas products to the export pipes. As a consequence of the oil and gas industry, large areas at the sea bed is covered with pipelines. [2]

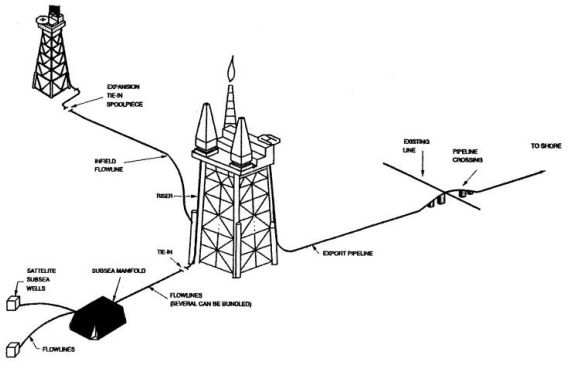

Figure 2.1: Example of flow lines offshore [2]

Since many subsea pipelines contain products from the offshore industry,

e.g oil, a leakage could result in an environmental disaster. Therefore, all risks need to be accounted for when designing pipelines. Loads from trawl equipment is one of these risks, as an interaction between pipeline and trawl equipment could lead to local bucking of the pipeline due to large bending moments in the material plastic area.

2.2 Trawling

Trawling is an important method for catching fish used in the fishing industry around the world, including Norway. The vessel performs a trawling process when it tows the fishing net with an opening in the direction of travel. A trawl is composed of a fishing net, called the trawl bag, which is attached to the vessel with a warp-line. There are three types of trawl systems, based on how the opening of the trawl bag is maintained [8]:

- Beam trawl
- Otter trawl
- Twin trawl

As the fishing vessel moves forward, water will pass through the mesh of the trawl bag, while fish above a certain size is unable to get through the mesh and thus get captured [8]. Trawling can be performed at all depths in the water column, depending on which species being fished. In this chapter the bottom trawl is in focus, as the main master thesis objective is clump weight pipeline interactions, and the interaction is occurring at or close to the sea bed.

2.2.1 Beam Trawl

The layout of a beam trawl is shown in figure 2.2. The beam trawl keeps the trawl bag open with a fixed transverse beam having one beam shoe at each end. This keeps the trawl opening in a fixed position. The beam trawl is normally used in a pair of two and is towed by outriggers on each side of the vessel. This trawl system is mainly used as bottom trawl gear. A big advantage with this beam trawl is that the trawl bag is kept open regardless of vessel speed. However, a disadvantage is that the height of the opening

is limited to about 1 m, making it unsuitable for most target species in Norwegian waters [8].

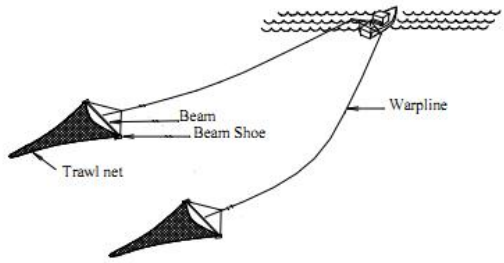

Figure 2.2: Beam trawl [5]

2.2.2 Otter Trawl

A layout of the otter trawl can be seen in figure 2.3. The otter trawl is equipped with trawl boards, one at each side of the trawl bag. The horizontal opening of the trawl bag is maintained by a hydrodynamic spreading force from the two trawl boards [5]. To ensure a satisfactory spreading of the trawl bag, it is necessary to connect sweep lines and warp lines at a suitable position on the trawl board. This is to obtain a proper angle of attack relative to the direction of travel [11]. Since the hydrodynamic spreading force ensures an opening in the trawl bag, higher velocities are required to produce a satisfactory spreading of the trawl bag [9]. The otter trawl is the most common bottom trawl used in Norwegian waters [9].

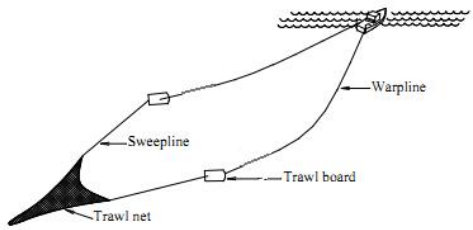

Figure 2.3: Otter trawl [5]

2.2.3 Twin Trawl

The configuration of a twin trawl including clump weight can be seen in figure 2.4 and 2.5. The twin trawl was developed in the last decades as an expansion of the otter trawl. The method is based on one single vessel towing two trawl bags side by side. When using two trawl bags, the catch rate and efficiency increase, hence the method is expected to increase in the future [17]. The twin trawl consists of a heavy clump weight between the two trawl bags at the end of centre warp line (figure 2.4). The clump weight, together with the trawl boards, keep the trawl bags separated and open due to hydrodynamic forces. A large share of the towing resistance is transferred to the centre warp line, resulting in a reduction of the necessary spreading force due to a reduction of tension in warp lines connected to the trawl boards. This leads to a larger trawl bag opening than for a single otter trawl and is the main advantage with using a twin trawl [9]. Since most of the warp line tension is transferred to the centre warp line, this also leads to an increased upward pull, hence the clump weight need to be heavy to resist this force. These clump weights are among the heaviest trawling equipment used and are normally between 2 to 9 tons [17].

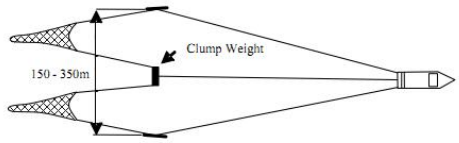

Figure 2.4: Twin trawl with clump weight [5]

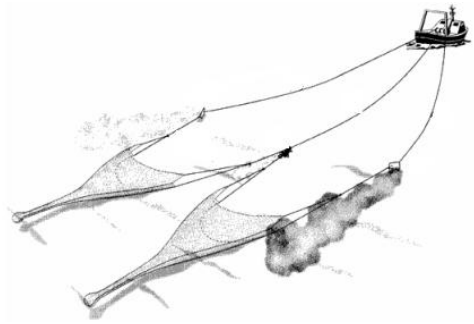

Figure 2.5: Twin trawl with clump weight [5]

There are several clump weight designs, ranging from just a bundle of chains to more special purpose designs. Two common clump weight designs are

bobbin clump weight and roller clump weight. A bobbin type can be seen in figure 2.6, and a roller type can be seen in figure 2.7. The bobbin clump weight is smaller and has lower weight than the roller type. Typically, the bobbin type weighs between 2 to 3.5 tons, while a roller clump weight can be up to 9 tons [17]. In the North Sea and the Norwegian sea, a clump weight mass up to 6 tons is common, while in the Barents sea trawling for prawns a clump weight mass up to 9 tons is used [17]. The pull over force from clump weight pipeline interaction is affected by the clump weight mass and height [5]. The bobbin type will therefore normally generate a lower pull over force than the roller type, thus it is concentrated on roller clump weight in the master thesis.

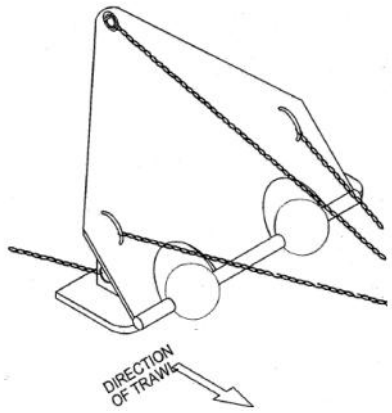

Figure 2.6: Bobbin type clump weight [5]

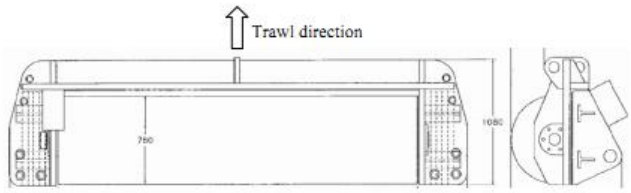

Figure 2.7: Roller type clump weight [5]

2.3 Current regulations

In the Norwegian sector requirements from the authorities state that all subsea installations shall not unnecessarily or to an unreasonable extent

impede or obstruct fishing activities [5]. Even if these requirements are met there is a need to design pipelines with trawl activities in mind, as subsea structures attract fish and thus fishing vessels. Historically, pipelines are protected against trawling impact by burying of the pipeline, gravel dumped onto the pipeline or pipeline coating [5]. However, these methods are expensive, and the demand for renewed design methods and practises arose. A recommended practice, focusing on interference between trawl gear and pipelines, was thus developed by DNV [5]. The recommended practice is abbreviated DNV-RP-F111, and is made as a guideline for pipeline design, to ensure a safe design.

The recommended practice states that bottom trawls need to be considered when designing offshore pipelines due to [5]:

- Possible hazard and inconvenience to the fishermen in case of trawl gear hooking to the pipeline
- Possible hazard to the integrity of the pipeline due to loads from the trawl gear

The master thesis, as well as the recommended practice, focus on the last condition. A trawl pull over load may cause lateral displacement and bending of the pipe. This could lead to a high utilization of the pipe steel material and/or local buckling of the pipe. There is a need to design pipelines in such a way that failure modes caused by large trawl equipment is avoided. The recommended practice differentiate between impact incidents in two phases and one special case [5]:

Impact phase

Defined as the initial impact phase where the trawl equipment first hit the pipeline. Trawl equipment could be trawl board, clump weight or beam shoe. This stage is normally lasting for some hundredths of a second. Resisting the impact force is mainly done by local resistance of the pipe shell, including eventual protective coating. [5]

Pull-over phase

Defined as the second stage where trawl equipment is dragged over the pipeline by the warp line. This phase is usually lasting between 1 to 10

seconds, depending among other factors on the water depth and span height [5]. This phase usually give a more global response of the pipeline.

Hooking

Defined as the state where the trawl equipment is stuck under the pipeline. The forces at the pipeline could in this occurrence be as large as the breaking strength of the warp line. Fortunately this situation is seldom occurring.

The recommended practise contains procedures when calculating impact force, pull-over force, critical hooking span height, acceptance criteria and coating impact testing. A dynamic analysis should be performed when calculating design load response from pull over trawl gear, applying the pull over force as a single point load [5]. Relevant non linearities, as non-linear material behaviour, soil resistance and buckling effects from effective axial force should be included in the analyses [5]. Pull over loads from the recommended practice are valid for low free span heights with pipeline diameters between 250 mm and 1000 mm, as long as the clump weight is of bobbin or roller type [5].

2.3.1 Use of recommended practice in design

When designing a pipeline it is important to consider pull over loads, checking if the load is below the pipeline threshold limit. DNV-RP-F111 presents a method for calculating pull over load. This method is based on a experimental model test executed at MARINTEK in 2004, with rigid pipelines [5]. The model test is described in detail in chapter 2.4. Pull over load calculations can only be used if the pull over force is not dominated by flexibility of potential free spans [5]. Maximum horizontal pull over force from clump weight pipeline interaction can be found as [5]:

$$F_p = 3.9 m_t g (1 - e^{-1.8h'}) (\frac{OD}{L_{clump}})^{-0.65} \tag{2.1}$$

$$h' = \frac{H_{sp} + OD}{L_{clump}} \tag{2.2}$$

Parameters used in equation 2.1 and 2.2 is explained with figure 2.8, where m_t is the steel mass, g is the gravity, OD is the outer diameter of pipe

included coating and L_{clump} is the distance from the reaction point to the centre of gravity of the clump weight.

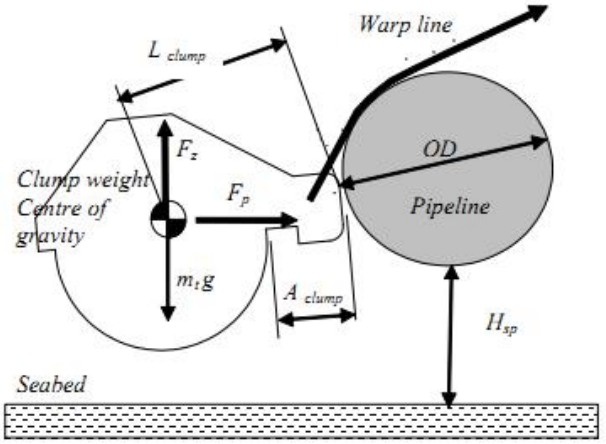

Figure 2.8: Clump weight pipeline interaction [5]

The maximum vertical pull over force is separated between maximum vertical upward and downward pull over force [5]:

$$F_z = 0.3F_p - 0.4m_t g \tag{2.3}$$

$$F_z = 0.1F_p - 1.1m_t g \tag{2.4}$$

Equation 2.3 gives the maximum upward vertical force and equation 2.4 gives the maximum downward vertical pull over force. Both equations depend on F_p. In each case it should be considered which vertical force gives the most critical load combination.

A clump weight pull over line of action can be described with three steps. First the clump weight stops just after impact. Secondly the warp line is tensioned. Thirdly, clump weight is pulling on the pipeline until the clump weight is rotated over the pipeline, ending the pull over interaction. According to [5], model tests show that dynamic load effects are not significant during pull over, thus the clump weight can be represented as a quasi static load. However, pipeline response may be dynamic, as in the case of global buckling.

The pull over duration is an important parameter in clump weight pipeline impact, as it is usually closely related to the pull over force. DNV-RP-F111 lists four parameters assumed to govern pull-over duration:

- Trawl velocity
- Pipeline induced movement at interaction
- Warp line stiffness
- Clump mass

Pull over duration can be calculated using the following equation [5]:

$$T_p = (\frac{F_p}{k_w V})(\frac{\delta_p}{V}) \tag{2.5}$$

k_w is the warp line stiffness, V the trawling velocity and δ_p the displacement of pipeline at point of interaction. δ_p is unknown at the beginning of the response analysis, and has to be assumed and further checked in an iterative procedure.

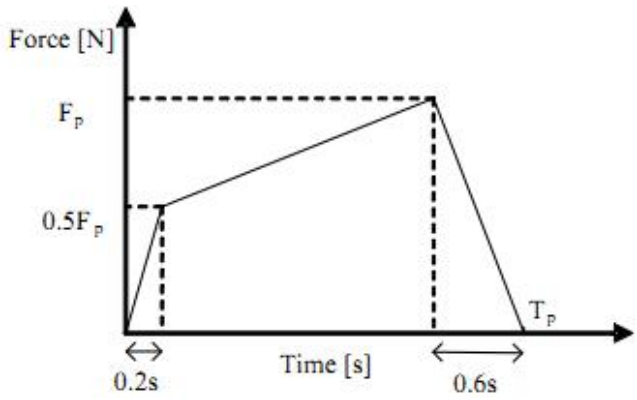

Figure 2.9: Force time history [5]

2.4 Clump weight experimental model test

In 2004 Statoil requested a model test investigating clump weight pull over forces on free spanning pipelines. This was carried out in association with development of the Kristin and Snøhvit oil and gas fields in the Norwegian sea. 139 tests were carried out in the ocean laboratory at MARINTEK [16].

The model test report, and later a document with all results, was made available to this master thesis for verification purposes. The recommended practice, DNV-RP-F111, is based on results from these model tests. A brief description of the model test will be given. The values given in this section are full scale values originating from the model test report [16]. A model scale of 1:10 was used, and all models was scaled according to Froude's law [16].

2.4.1 Trawl gear

The twin trawl gear, including trawl net, warp lines, sweep lines, clump weight and trawl boards, was provided from SINTEF fisheries and aquaculture, in Hirtshals, Denmark. Trawl nets and sweep lines were included in the test to ensure a correct drag and mass, securing a correct back tension to the trawl boards and clump weight. The upper ends of the warp lines were fixed to a towing carriage. The outer warp lines were connected to trawl boards, while the centre warp line was connected to the clump weight. It was 350 m water depth, and a warp line length of 895 m was chosen to represent a warp line angle of 23 °. The warp line included springs at its upper ends to simulate the correct stiffness. With regard to later re-computations, two warp line stiffnesses were used, namely 30 kN/m and 60 kN/m. [16]

The type of trawl board used, was a model scale version of a Thyobrøn 135" door weighing 3.8 tons each. Two different clump weights were used, namely the bobbin type and the roller type, see figure 2.10 and 2.11. The Thyobøn roller type clump weight had a dry weight of 6.1 tons, while the bobbin type had a dry weight of 3.6 tons.

Figure 2.10: Bobbin type clump weight

Figure 2.11: Roller type clump weight

2.4.2 Free spanning pipelines in model test

Three pipelines, with diameters 350 mm, 530 mm and 840 mm, were modelled from steel pipes. To obtain the proper mass, the pipes were ballasted with a combination of lead, foam and water. The span height varied between six different heights: 0.0 m, 0.25 m, 0.5 m, 0.75 m, 1 m, and 4 m, and pipe end conditions were varied between fixed, flexible and trenched. The total length of the modelled pipelines were 25 m. Pipe ends were sealed with steel lids and prepared for mounting to the test rig force transducers. [16]

Force transducers were fixed to each end of the pipeline to measure forces parallel to the towing direction (horizontal transversal forces) and forces in vertical direction. Pipe deflection measurements were performed by a calibrated combined spring and strain gauge tension ring system placed between the pipe ends and the end frame at both ends. Pipe deflection was measured in horizontal direction. A pre calibrated adjustable damper and a set of linear springs were placed at each side of the pipeline between the end frame and the pipeline. [16]

2.4.3 Test procedure

For each test the procedure can be described in the following way [16]:

- Twin trawl laid out on the bottom in starting position.
- Test rig made ready.
- Start of recording and towing.
- Stabilization of tow with trawl gear into wanted towing position at constant speed.
- Towing of clump weight across the pipeline and measuring interaction loads.

- Stop of towing carriage, return of trawl gear to initial position.

The test procedure was executed for four different towing velocities, depending on the clump weight type. The Thyborøn clump weight type was carried out with following velocities: 1.45 m/s, 1.75 m/s, 1.95 m/s and 2.18-2.45 m/s.

2.4.4 Test results

Horizontal and vertical pull over force, warp line tension and pipeline horizontal displacement were measured. The data was presented as time histories. All force and displacement histories were low pass filtered at 1.58 Hz to remove signal vibrations from the result. The main findings can be summarised with [16]:

- Horizontal pull over force increased with increasing span height, for all pipe diameters.
- Horizontal pull over force decreased with increasing pipe diameter.
- Horizontal pull over force was greater for the 6.1 ton roller type clump weight, than with the 3.6 ton bobbin type.
- Warp line tension seemed to follow the same pattern as the horizontal pull over forces.
- Vertical pull over forces were an order of magnitude smaller than the horizontal pull over forces.

2.5 Previous work on trawl gear pipeline interactions

Earlier, some master theses have been written on the same and similar topics. One is a master thesis written in 2009 by Martin T. Møller. His master thesis focused on pull over loads from polyvalent trawl boards, where the effect of variation in span heights and trawling velocities has been performed using SIMLA [14]. Results are compared with belonging design loads calculated from DNV-RP-F111. For high free span heights, he found satisfactory similarities between simulation pull over forces and design loads. The effect of increased trawl speed from 2 m/s to 3 m/s was found to be smaller for the simulation forces than for the design loads. In several

analyses he found deviations from the design load, and an uncertainty concerning the computer model created.

In 2010, Vegard Longva wrote a master thesis also focusing on trawl board pipeline interaction. Among other factors he examined oblique trawl board crossings, finding that a perpendicular crossing did not predict the largest pull over load in all incidents. He also made a new hydrodynamic load model including effect of forward speed and seabed proximity, to simulate perpendicular trawl board crossings. [11]

During the spring of 2011, Kristian Maaløe wrote a master thesis focusing on clump weight pipeline interactions. He developed input files based on the experimental model test, and analysed the input files using SIMLA. He completed simulations for three different free span heights and focused on a 350 mm pipe diameter case. The main finding of the master thesis was that an increase in pipeline flexibility resulted in a decrease in pull over forces [12]. When simulation results were compared to design loads calculated from DNV-RP-F111, simulation pull over loads were found considerably lower in both duration and magnitude [12].

In the fall of 2011, I wrote a preliminary project on clump weight pipeline interactions, investigating speed variation dependency. One input model with 350 mm pipe diameter, 0.75 m free span flexible condition, developed by Kristian Maaløe, was used as a base for the simulations. The main finding was that the pull over force, and especially pull over time increased with decreasing towing speed. Additionally, a dependence between pull over force and free spans were found, where a lower free span resulted in lower pull over force.

2.6 Scope of work

In the master thesis, simulations with clump weight pipeline interaction is performed in the finite element program SIMLA.

The decision to use an input model developed by Kristian Maaløe as a foundation for developing new cases was made in agreement with my supervisors. It had already been shown that simulations from this model was in agreement with some model test results. Thus, it would be unnecessary to develop a new model with the same properties. However, it would be interesting to expand the input file and investigate new cases within the same foundation. Several alterations had to be made, but the

geometry and element classification were principally the same. The models provided were one experimental test model with 350 mm pipeline diameter flexible condition 0.75 m free span and one full scale model with 350 mm pipeline diameter 0.75 m free span.

Results from SIMLA can be compared with model test results, when having similar clump weight pipeline configurations. Investigating whether or not the same trends are shown in both the model test and the computer analyses results are of interest.

The main focus of the master thesis has been to find out more about which parameters in clump weight pipeline interaction is important when small or bigger changes are introduced. The experimental test model was expanded to apply for 530 mm and 840 mm pipeline diameter. An investigation to see if these simulations corresponded good with model test results were conducted. Another area of interest was to look into the effect of introducing flexibility in the model and how this relates to the design load, which is based on model tests with a rigid pipeline. All simulations are compared to the corresponding model test results and design loads, calculated from DNV-RP-F111.

Chapter 3

Non-linear finite element analysis

The finite element method, from here on FEM, is a numerical method where differential equations are solved approximately [18]. FEM is the main analysis tool and is used to solve a wide variety of problems that are too complicated to be solved by analytical methods. Examples include structural analysis, heat transfer or fluid flow. When creating a finite element model, a discretization of that model is executed. The essence of FEM is that a complicated problem can be divided into small elements that is solved in relation to each other, making the analysis easier [15]. The special purpose computer program SIMLA is based on this method. This chapter is an introduction to finite element method. An area of interest will be on structural FEM in general, but also on non-linear finite element methods used in SIMLA. The reason for using a special purpose finite element program when analysing clump weight pipeline interactions is due to its capability capturing the complexity of the problem and compute realistic response.

A finite element analysis can be divided into three steps [3]:

- Preprocessing
- Numerical analysis
- Post processing

During preprocessing, an input file is created which describes the geometry with element and nodal arrangements, boundary conditions, material

properties and loads for the current problem. Mesh density is also indicated for each type of element. When running a time domain analysis, time steps needs to be defined. Wanted results will also need to be defined. FlexEdit is used in the preprocessing part.

SIMLA is used for the numerical analysis step. During this step the software will automatically generate matrices to describe the behaviour of each element, and combine the matrices into a large matrix equation representing the finite element structure [3]. The equation is solved and the nodal and elemental requested values are computed. The analysis is non-linear and solved in time domain.

During post processing, the output files from SIMLA are read directly by the post processing program and results are shown. This is done in a visualisation program creating graphs from the list of results, or in a 3D simulation program which also simulate the results. Xpost is used as a post processing program, which are able to simulate the analyses in 3D. Finally MATLAB is used to automatically generate the graphs used in this report by creating a script of functions.

A final check of the results are necessary to see if they are reasonable. If errors are investigated a re-run has to be done, troubleshooting the input files, e.g checking mesh density.

3.1 Basic finite element principles

For all finite element analyses, both linear and with some adjustments non-linear problems, three basic principles need to be complied with [15]:

- Equilibrium
- Kinematic compatibility
- Stress-strain relationship

All three principles will be described in more detail in the following section.

3.1.1 Equilibrium

Work done by internal stresses should be equal to external forces. This could be obtained by solving the differential equilibrium equation [15]. However, the exact equilibrium equation is in many cases impossible to solve, and

often approximations are necessary. In SIMLA the principle of virtual displacements is used to obtain an approximate solution [20]. The basic idea of this approximation is to in average fulfil the differential equation by weight function multiplication and volume integration, as an alternative method of finding the exact solution [20]. The computed work is artificial, done by forces and stresses due to virtual displacements and virtual strains. The stresses and displacements do not need to represent the true distribution in the deformed structure, and they can be independently given. [15], [20]

A structure exposed to a virtual displacement field satisfying boundary conditions, will lead to a situation where the internal work and external work are zero in an averaged sense [20]. A state of integrated equilibrium is obtained, with zero error in average. The equilibrium is however not necessary fulfilled at a random point in the volume. In SIMLA initial stresses are included while volume forces are not [20]:

$$\int_V (\rho\ddot{\mathbf{u}} - \mathbf{f}) \cdot \delta\mathbf{u} dV + \int_V (\sigma - \sigma_{\mathbf{0}}) : \delta\varepsilon dV - \int_S \mathbf{t} \cdot \delta\mathbf{u} dS = 0 \tag{3.1}$$

ρ is the material density, $\ddot{\mathbf{u}}$ is the acceleration field, $\mathbf{f}$ is the volume force vector, σ is the stress tensor of Cauchy stress, $\sigma_{\mathbf{0}}$ is the initial stress tensor, ε is the strain tensor of natural strain, $\mathbf{t}$ is the surface traction and $\mathbf{u}$ is the displacement vector.

3.1.2 Kinematic compatibility

Kinematic compatibility is taken into account by assuring that the approximation of the deformation is continuous over element boundaries, and making sure that the assumed displacement field is compatible with the strain field. This is obtained by describing displacements with continuous interpolation functions and ensuring that strains are finite at element boundaries. [15], [3]

In SIMLA, kinematic compatibility for a pipe element is based on the assumption that the Bernoulli-Euler hypothesis is applicable [20]. The hypothesis states that plane cross-sections normal to the neutral axis, remain plane and normal to the neutral axis throughout deformation. When formulating incremental equilibrium equations, a green strain tensor is used. The longitudinal Green strain, when focusing on an elastoplastic pipe element and neglect shear deformations and 2nd order longitudinal strain, can be written as [20]:

$$E_{xx} = u_{,x} - yv_{,xx} - zw_{,xx} + \frac{1}{2}(v_{,x}^2 + w_{,x}^2) + \theta_{,x}(yw_{,x} - zv_{,x}) + \frac{1}{2}\theta_{,x}^2(y^2 + z^2) \quad (3.2)$$

In the master thesis linear pipe elements were used. In equation 3.2 u, v and w are the displacement in x, y and z direction respectively, and θ is the torsion rotation of the neutral axis. By including equation 3.2 in the equilibrium equation, the compatibility requirement in finite element is automatically fulfilled [20].

3.1.3 Stress-strain relationship

In SIMLA the user can choose between elastic and elastoplastic material. The elastic stress-strain relationship for a pipe element can be expressed by the following Hooks expression [20]:

$$\begin{bmatrix} \sigma_{11} \\ \sigma_{22} \\ \tau \end{bmatrix} = \frac{E}{1-\nu^2} \begin{bmatrix} 1 & \nu & 0 \\ \nu & 1 & 0 \\ 0 & 0 & \dfrac{1-\nu^2}{2(1+\nu)} \end{bmatrix} \begin{bmatrix} \varepsilon_{11} \\ \varepsilon_{22} \\ \gamma \end{bmatrix} \quad (3.3)$$

The elastoplastic material formulation is needed if stresses exceed yield stress in the material. This is because the strain in plastic materials are separated into two parts [15]:

$$d\varepsilon = d\varepsilon^e + d\varepsilon^p \quad (3.4)$$

The elastic strain is still calculated based on the elastic material law, but the plastic strain need to be found. There are three main contributions, called the constitutive laws, which need to be taken into account dealing with plasticity:

Yield criterion

Defines the stress state where plastic deformation first appears. The yield condition can generally be expressed in terms of the yield function, f. By defining f equal to zero, the yield surface is defined [15]:

$$f(\sigma_{ij}, \varepsilon_{ij}^{p}, \kappa) = 0 \tag{3.5}$$

for all σ_{ij} and ε_{ij}^{p} components. κ is a strain hardening parameter.

The domain of the yield surface is defined as [15]:

- $f < 0$; elastic state of stress
- $f = 0$; plastic state of stress
- $f > 0$; inadmissible

Hardening rule

Describes, as yield continues, a modification of the yield condition due to strain hardening [15]. In SIMLA, both kinematic and isotropic hardening are included, and you are able to choose between the two hardening models. The difference between the two become apparent when loading is reversed, see figure 3.1.

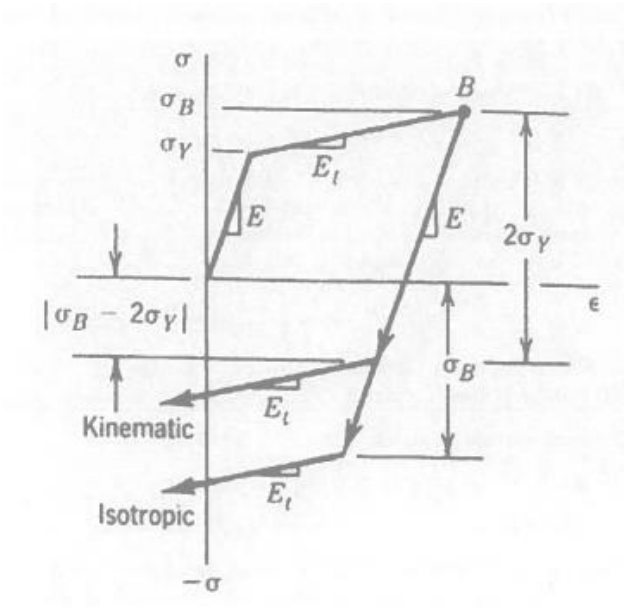

Figure 3.1: Kinematic and isotropic hardening, uni axial state of stress [20]

In isotropic hardening, the yield criterion is unchanged when loading is reversed. If this does not comply with the relevant material, kinematic

hardening can be used. In kinematic hardening an elastic range equal to $2\sigma_y$ is preserved. Kinematic hardening gives an effect called the Bauchinger effect, meaning that the yield capacity during unloading is less than initial capacity [15].

Flow rule

The flow rule allows plastic strain increment determination at each point in the load history, and yields an incremental relationship between Cauchy stresses and true strains [15]. For small strains, the same can be said about Piola-Kirchhoff stresses and Green strains.

This is obtained by first assuming a valid yield criterion. The next assumption is that the Drucker's postulate is valid. This implies that[15]:

- The yield surface is convex
- The plastic strain increment is normal to the yield surface
- The plastic strain increment is a linear function of the stress increment

The result of the flow rule gives the incremental stress-strain relationship [15]:

$$d\sigma_{ij} = E_{ijkl}(d\varepsilon_{kl} - d\varepsilon^p_{kl}) = D^{ep}_{ijkl} d\varepsilon_{kl} \tag{3.6}$$

3.2 Non-linear effects

In a non-linear structural problem one need to account for non linearities that is affecting the structure. For a clump weight pipeline interaction, non-linearities are highly present. They can for instance be found during pipeline-seabed contact, or in large deflections of pipeline due to interaction. Contact problems are in general non-linear problems, due to sudden changes in contact, which often result in quick changes in stiffness [15]. The non-linearities are divided into three sub-categories [3]:

3.2.1 Geometry non-linearity

Geometrical non-linearity has to be taken into account when deformations are large, allowing for a change in equilibrium equations with regard to the

deformed structural geometry, by calculating strains from displacements [15]. This modification is apparent a necessity when computing buckling and collapse load. In clump weight pipeline interaction analysis this can be found in pipeline deflection during interaction.

3.2.2 Material non-linearity

Material non-linearity appear when material properties are functions of the state of stress or strain, e.g when experiencing plasticity [3]. This means that Hooks law is no longer valid and a non-linear stress-strain relationship need to be taken into account [15]. This is done by the constitutive laws described in chapter 3.1.3.

3.2.3 Boundary conditions

Non linear boundary conditions can be associated with contact problems. This can occur if large displacements lead to contact, e.g if two surfaces come into or out of contact. Displacements and stresses of the two contacting structures are usually not linearly dependent on the applied loads [15].

3.3 Finite element formulation

When formulating the finite element method for a structural non linear geometrical problem, it is necessary to choose a reference system describing the geometry and deformations in the structure. It is common to distinguish between two methods, namely the Total Lagrangian formulation (TL) and the Updated Lagrangian formulation (UL), although other methods are available. [20]

The Total Lagrangian formulation is based on a fixed coordinate system, where all static and kinematic variables are referred back to the initial non-deformed configuration, C_0 [20]. While the Updated Lagrangian formulation refers to the last step, i.e. the last attained equilibrium configuration, C_n [20]. In figure 3.2 the Total Lagrange method uses C_0 as a reference, while the Updated Lagrange method uses C_n as a reference.

In SIMLA, a variation of the updated Lagrange method is used, called the Co-rotational formulation [20]. The basic idea with Co-rotational

formulation is to separate rigid body motions from the local deformation of the element so that non-linearities from large displacements can be separated from non-linearities within the element [20]. This is solved by fixing a local coordinate system to the element, being updated continuously as the element deforms. In figure 3.2, the Co-rotational formulation will have C_{0n} as a reference.

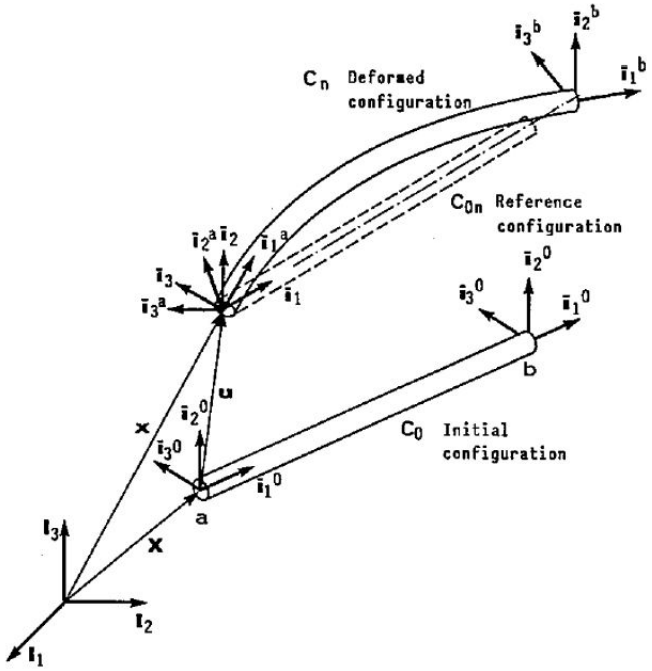

Figure 3.2: Reference configuration, motion of beam nodes [13]

3.4 Solution method

The basic principle in structural analysis solution solving, is to make sure that equilibrium between external forces and internal mass, damping and reaction forces are fulfilled [15]:

$$\mathbf{R_{ext}} - \mathbf{R_{int}} = \lambda \mathbf{R_{ref}} - \mathbf{R_{int}} = \mathbf{0} \tag{3.7}$$

In SIMLA, both static and dynamic analysis can be used to solve the equilibrium equation.

3.4.1 Static solution method

In SIMLA, the static solution method is based on Newton-Raphson equilibrium iteration at each load step. The Newton-Raphson method can be described with the following equation: [20]

$$\mathbf{\Delta r^{i}_{k+1}} = \mathbf{K^{-1,i}_{T,k+1}} \mathbf{\Delta R^{i}_{k+1}} \tag{3.8}$$

$\mathbf{K_T}$ is the tangential stiffness matrix, $\mathbf{r}$ is representing displacements, and the index k is referring to the current load step number. The Newton Raphson method can be seen in figure 3.3 where the load increment ΔR results in a displacement increment Δr at iteration 0. The iteration continues until convergence is realised, hence the unbalanced term $\delta r_k = 0$. [20]

3.4.2 Dynamic solution method

In the analyses presented in this master thesis, a dynamic solution procedure is used. The dynamic solution procedure makes use of a direct time integration of the equation of motion. This is essential as non linear dynamic problems are unable to be solved by modal superposition. [20]

The direct time integration can be solved by an explicit or an implicit method.

Explicit method

If displacements at time step t+Δt can be solved by use of known parameters from the last time step it is called an explicit method, see equation 3.9 [15]. Small time steps must be used, as explicit methods are conditionally stable.

$$\mathbf{r_{k+1}} = \mathbf{f}(\mathbf{\ddot{r}_k}, \mathbf{\dot{r}_k}, \mathbf{r_k}, \mathbf{\ddot{r}_{k-1}}, ...) \tag{3.9}$$

When dealing with an impulse response it is important to use small time steps to capture the whole load history and obtain satisfactory accuracy. Due to this fact explicit methods are normally used for impact problems.

Implicit method

In an implicit method, displacements depend on parameters found in the next time step in addition to previous load steps, see equation 3.10 [15].

$$\mathbf{r_{k+1}} = \mathbf{f}(\ddot{\mathbf{r}}_{\mathbf{k+1}}, \dot{\mathbf{r}}_{\mathbf{k+1}}, \ddot{\mathbf{r}}_{\mathbf{k}}, \dot{\mathbf{r}}_{\mathbf{k}}, \mathbf{r_k}...) \tag{3.10}$$

As implicit methods include information from the next time step, they will be more numerically stable than explicit methods. The different implicit methods are distinguished from each other by how accelerations are assumed to vary between time steps, and when the equilibrium equation is fulfilled [20]. If assuming a constant average acceleration, this will result in an unconditionally stable method where numerical stability is provided, unaffected of time step size [20]. As a result it is favourable to use this kind of methods when long duration analyses are performed. However, with implicit methods one need to solve the coupled equation system at each time step, making this method undesirable if short time steps are needed due to accuracy. [20]

In dynamic analyses we are interested in the lower eigenmodes with the highest accuracy, and not high frequency modes with low accuracy [20]. As a consequence an effort is made to remove higher modes in the system. This can be done by introducing the Newmark-ß method, where introducing rayleigh-damping or increasing the damping ratio results in damping of the medium modes while the lower and higher modes remains nearly unchanged [20]. Higher modes, however, can be damped out by numerical damping. This leads to a reduction of accuracy from 2nd to 1st order. To avoid this reduction in accuracy, another method could be implemented; the HHT-α method. This implicit method is used in SIMLA as an incremental time integration method, and can damp out higher frequency modes but still remain 2nd order accuracy. [20], [13].

3.4.3 Incremental time integration system

To carry out an incremental time integration system in SIMLA, the HHT-α method is utilized. This method use the same approximations as in the Newmark-β method to find accelerations an velocities at time step k+1 [20]:

$$\Delta\ddot{r}_{k+1} = \Delta\ddot{r}_{k+1} - \Delta\ddot{r}_k = \frac{1}{\Delta t^2\beta}\Delta r_{k+1} - \frac{1}{\Delta t\beta}\dot{r}_k - \frac{1}{2\beta}\ddot{r}_k \tag{3.11}$$

$$\Delta\dot{r}_{k+1} = \Delta\dot{r}_{k+1} - \Delta\dot{r}_k = \frac{\gamma}{\Delta t\beta}\Delta r_{k+1} - \frac{\gamma}{\beta}\dot{r}_k - \Delta t(\frac{\gamma}{2\beta} - 1)\ddot{r}_k \tag{3.12}$$

Where Δt is the time step, γ and β are integration parameters. However, the equilibrium equation is modified when using HHT-α method [20]:

$$\mathbf{M}\ddot{\mathbf{r}}_{k+1} + (1+\alpha)\mathbf{C}\dot{\mathbf{r}}_{k+1} - \alpha\mathbf{C}\dot{\mathbf{r}}_k + (1+\alpha)\mathbf{R}^I_{k+1} - \alpha\mathbf{R}^I_k = (1+\alpha)\mathbf{R}^E_{k+1} - \alpha\mathbf{R}^E_k \tag{3.13}$$

Here α is the α-parameter, k refers to the current time step, and $k+1$ the next time step. $\mathbf{M}$ is the mass matrix, $\mathbf{C}$ is the damping matrix, $\mathbf{R}^I$ the internal force vector and $\mathbf{R}^E$ the external force vector. $\mathbf{C}$ consists of both Rayleigh damping and a diagonal damping matrix [20].

With a smaller value of α, more damping is implemented in the numerical solution. If $\alpha = 0$ the Newmark-β method is obtained.The HHT-α method will meet the 2nd order accuracy and stability if α, β and γ has the following values [13]:

$$-\frac{1}{3} < \alpha < 0$$

$$\gamma = \frac{1}{2}(1 - 2\alpha)$$

$$\beta = \frac{(1-\alpha)^2}{4}$$

By subtracting all components in time step k from the equilibrium equation (equation 3.13) a relation between the stiffness, displacements and loads can be found: [13], [20]

$$\hat{\mathbf{K}}_k\Delta\mathbf{r}_{k+1} = \Delta\hat{\mathbf{R}}_{k+1} \tag{3.14}$$

$\hat{\mathbf{K}}_k$ is the effective stiffness in time step k, and $\Delta\hat{\mathbf{R}}_{k+1}$ is the effective load vector.

The equation for the effective load vector, $\Delta\hat{\mathbf{R}}_{k+1}$, detects and adjust any unbalanced forces at the current time step, k, and ensures that an eventual unbalance in equation 3.13 does not accumulate [13].

Displacements at the next time step, $k+1$, can be found solving equation 3.14. Further, the acceleration and velocity is found from equation 3.11 and 3.12. The solution found, is normally not able to fulfil the equilibrium equation (equation 3.13) straight away. For this reason, performing iterations are usually necessary before moving to the next time step, $k+1$. [20]

3.4.4 Equilibrium iteration method

When iterating to make sure that the equilibrium equation (equation 3.13) is fulfilled, one can use several methods. The Newton-Raphson iteration method is used in SIMLA.

In pure Newton-Raphson, the tangent stiffness $\mathbf{K}_T$ contained in $\hat{\mathbf{K}}$, is updated at each iteration step, thus improving the convergence rate. If this is not done, the method is called modified Newton Raphson. See figure 3.3. In SIMLA, the governing iteration equation can be written as [20]:

$$\hat{\mathbf{K}}_k^i \delta \mathbf{r}_{k+1}^{i+1} = (1+\alpha)[\mathbf{R}_{k+1}^E - \mathbf{R}_{k+1}^{I,i} - \mathbf{C}\dot{\mathbf{r}}_{k+1}^i] - \mathbf{M}\ddot{\mathbf{r}}_{k+1}^i - \alpha(\mathbf{R}_k^E - \mathbf{R}_k^I - \mathbf{C}\dot{\mathbf{r}}_k^i) \tag{3.15}$$

The right hand side of equation 3.15 makes up for the unbalanced inertia, damping and internal forces. The acceleration and velocity increments are found from equation 3.11 and 3.12. The subscript i represents the iteration cycle number at step $(k+1)$. The total incremental iteration can be summarised with the following equations [20]:

$$\Delta \mathbf{r}_{k+1}^{i+1} = \Delta \mathbf{r}_{k+1}^i + \delta \mathbf{r}_{k+1}^{i+1} \tag{3.16}$$

$$\Delta \dot{\mathbf{r}}_{k+1}^{i+1} = \Delta \dot{\mathbf{r}}_{k+1}^i + \frac{\gamma}{\Delta t \beta} \delta \mathbf{r}_{k+1}^{i+1} \tag{3.17}$$

$$\Delta \ddot{\mathbf{r}}_{k+1}^{i+1} = \Delta \ddot{\mathbf{r}}_{k+1}^i + \frac{\gamma}{\Delta t^2 \beta} \delta \mathbf{r}_{k+1}^{i+1} \tag{3.18}$$

When equilibrium is achieved, the right hand side of equation 3.15 vanishes [20].

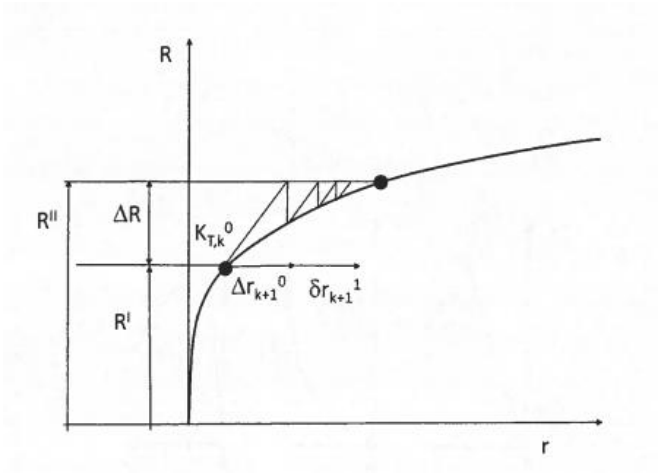

(a) Modified Newton-Raphson

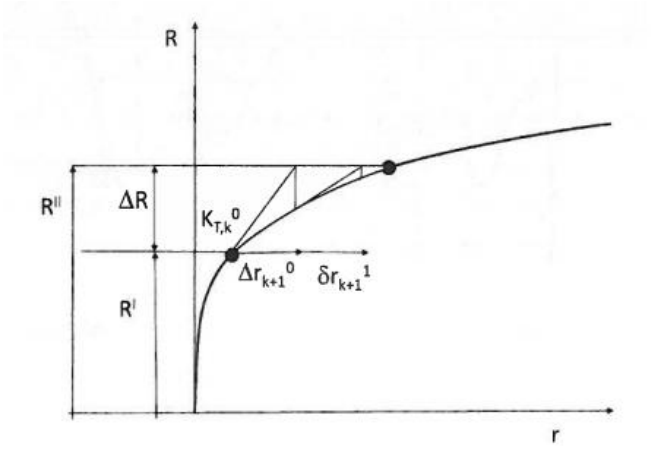

(b) Pure Newton-Raphson

Figure 3.3: Newton-Raphson iteration

3.4.5 Convergence criteria in equilibrium iteration

The convergence criteria ensures a desired level of accuracy. This is done by stopping the iteration when an accepted tolerance level is reached. In SIMLA, a fixed number of iterations are performed. If equilibrium is not met, the time step is divided before a new iteration is started. The convergence criteria can be based on total displacements, and is specified by the following equations: [20]

$$\|\delta \mathbf{r}_{k+1}^{i+1}\| < \epsilon_D \|\mathbf{r}_{k+1}^{i+1}\| \tag{3.19}$$

$$\|\mathbf{r}_{k+1}^{i+1}\| = \frac{1}{N}\sqrt{\sum_{j=1}^{N}(r_j^{i+1})^2} \tag{3.20}$$

$$\|\mathbf{r}_{k+1}^{i+1}\| = \|\mathbf{r}_{k+1}^{i+1}\| - \|\mathbf{r}_{k+1}^{i}\| \tag{3.21}$$

Equation 3.19 gives the tolerance level, controlled by the ϵ_D-parameter. This parameter has values normally in the order 10^{-2} to 10^{-6} [20]. In SIMLA, it is also possible to use energy or forces to specify the tolerance.

Chapter 4

FE analysis of clump weight pipeline interaction

All analyses in this master thesis are carried out using the finite element program SIMLA. SIMLA is a special purpose non-linear static and dynamic analysis program developed by MARINTEK, where the load and analysis series are described using time domain. The computer program is used for pipeline structures related to design, installation and operation. [19]

The SIMLA input files are based on Kristian Maaløs work, which have been further developed for the master thesis. Chapter 4 includes a description of the different simulation analyses and its input data. Three different SIMLA models were established and analysed:

- One model based on the experimental model test performed at MARINTEK in 2004. This model is referred to as "experimental test model".
- One real case pipeline model called "full scale model".
- One point load model used to compute design loads from DNV-RP-F111.

All three models have the same clump weight properties, and somewhat alike pipeline cross sectional geometry. However, the pipeline used in model tests are scaled down to such an extent that when reconstructing for simulating purposes, the pipe stiffness need to be very high to keep the same characteristics. For this reason, the pipeline in the experimental test model is considered rigid, while the full scale pipeline with real pipe

stiffness and other properties are more realistic. As the full scale pipeline has a lower axial stiffness and bending stiffness than the experimental test pipe, it will have a higher bending flexibility. The full scale pipeline is 1000 m long, while the experimental test model pipeline is 25 m.

One point load model was made for the experimental test model and one for the full scale model. The point load model was used to find the design load and was identical with the belonging simulation, except that trawl equipment was replaced with the point load having point of action at pipe mid span. Since design load equations developed by DNV are based on the experimental model test results, it is of interest comparing results from the two methods. In addition, a comparison between design load and simulated results is of interest, including both experimental test simulated results and results from the full scale model.

Experimental test model simulations were run for three different pipe cross section diameters, namely 350 mm, 530 mm and 840 mm, and three different free span heights, 0.75 m, 0.5 m and 0.25 m. The full scale model was analysed for two different pipe cross section diameters, 530 mm and 350 mm, and three different free span heights, the same as in the experimental test model simulations. The model test did execute some runs with 0 m free span, but it was however decided in collaboration with supervisors that the 0 m free span case could be skipped in the master thesis. The decision is based on several factors, one of them being a demand for change and increase of contact elements at more parts of the clump weight.

The objective for simulating the experimental test model is to reproduce model tests numerically, and analyse the response from clump weight over-trawling pipelines. From the results, a differentiation in the importance of different parameters can be established. The full scale pipeline model is analysed, comparing results to design loads to see if the current regulations are satisfactory and investigating the effect of a detailed free spanning pipeline regarding pull over forces.

4.1 Trawl gear

The trawl gear configuration is the same as in the experimental model test performed at MARINTEK in 2004 with a Thyborøn roller clump type. All input data is collected from the model test report and from the master thesis written by Kristian Maalø [16] [12]. The trawl gear configuration is

not altered between the different simulations, except in certain sensitivity studies where this is indicated.

4.1.1 General trawl gear data

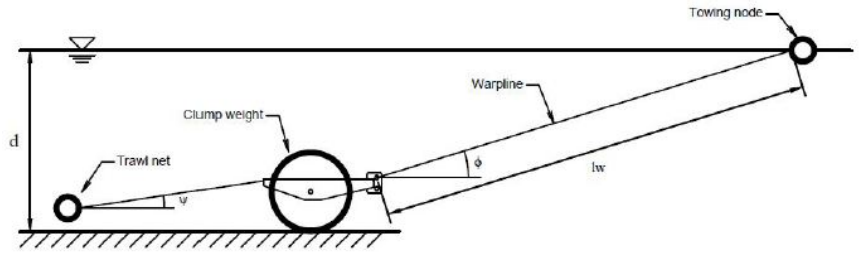

Figure 4.1: Trawl gear configuration, vertical plane

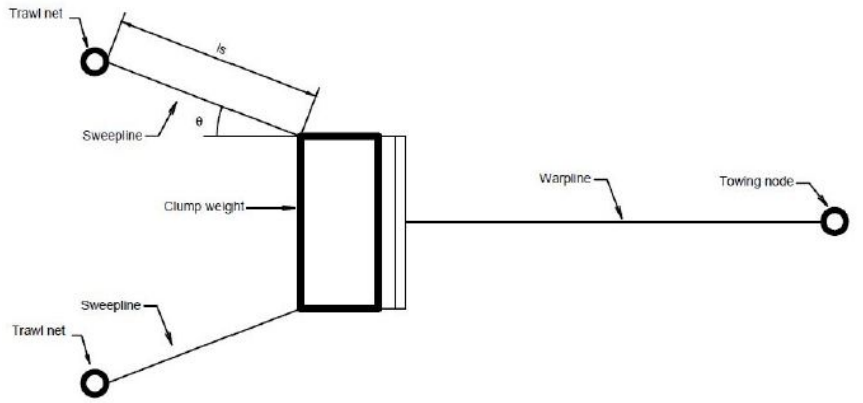

Figure 4.2: Trawl gear configuration, horizontal plane

The clump weight is pulled by a warp line going to the sea surface. In the end of the warp line at sea surface there is a towing node which is gradually accelerated up to 1.95 m/s by applying a defined time-displacement curve. Behind the clump weight there is two sweep lines with a drag node in the end of each line. The drag node is representing the trawl net with a fixed drag coefficient, but without mass. The drag coefficient was decided based on the model test, so that the tension in the warp line during constant towing corresponded to the measured warp line tension in the model test [12]. The trawl nets are modelled without mass to avoid compression forces in the sweep lines during impact. A sweep angle of 20° was assumed for

all simulations. Also, a vertical sweep angle of 0.3° was applied to account for the 18" steel bobbins, dragging the sweep line down between the sweep lines and the trawl nets. A table with general input values is presented in table 4.1. [12], [16].

Description	**Symbol**	**Value**	**Unit**
Depth	d	349	m
Trawling Velocity	V	1.95	m/s
Warp angle	ϕ	23	deg
Sweep angle	θ	20	deg
Vertical sweep angle	ψ	0.3	deg
Trawl net drag coefficient	C_d	20.8	m^2
Trawl net dry mass	m_d	0.0	kg

Table 4.1: General trawl gear data

The trawl gear configuration can be seen in figure 4.1 and 4.2.

4.1.2 Clump weight

The clump weight modelled in SIMLA is a Thyborøn roller type, closely related to the clump weight used in the model test. In this master thesis dimensions and mass distribution are obtained from the master thesis written by Kristian Maalø [12]. Originally, measurements of a similar clump weight scale model were obtained from SINTEF Fisheries and aquaculture, Hirtsharls, Denmark, as the values from the MARINTEK report were somewhat vague [12], [16].

According to SINTEF, the clump weight had a total dry mass of 3840 kg and a roller length of 1.55 m [12]. A figure and data of this clump weight is found in appendix A and B. SINTEF stated that no additional ballast weights were delivered. It is assumed that ballasting to 6100 kg was performed at site and placed inside the hollow roller. The pull over load is influenced by the mass distribution. Therefore the mass of the front frame part was placed separately along a front beam, while the remaining mass was assumed to act along the center line of the clump weight roller [12]. See figure 4.3.

The geometry cross sectional properties were originally taken from design drawings provided by the manufacturer, Thyobøn Skipsmedie AS, Denmark [12]. The design drawing can be seen in appendix A. The geometry is a bit simplified in the simulations, where the clump weight is modelled with a

clump weight roller, a frame and a warp line bracket. The layout can be seen in figure 4.3 and 4.4. Simplifications are done as they are believed to have minor effect on the pull over result, and they will simplify the analyses and input files. The clump weight was modelled with rigid linear pipe elements, assuming that no deformation and no dissipation of energy will take place in the clump weight during impact. The clump weight roller is 1.55 m long, modelled with two pipe elements with a diameter of 0.76 m. The roller was attached to the frame by constraints allowing the roller to rotate during towing. Vertical extensions of the frame was not taken into account, as it is assumed that only the lower part of the frame will be in contact with the pipeline. The warp line bracket is modelled with one pipe element, where the length is equal to the vertical straight edge of the warp line bracket from the design drawing, see figure 4.3. [12]

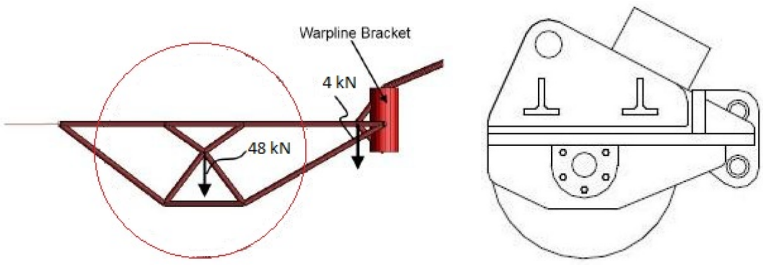

(a) Model used in SIMLA (b) Thyobøn design drawing

Figure 4.3: Clump weight comparison with design drawing from the side

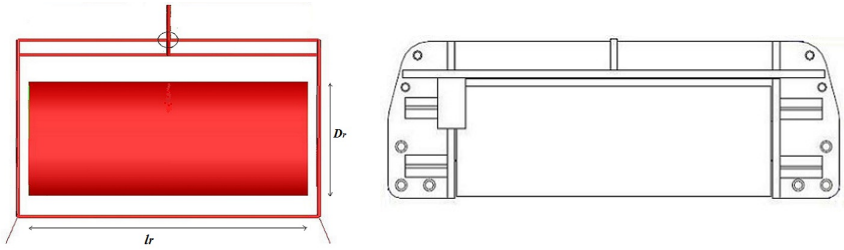

(a) Model used in SIMLA (b) Thyobøn design drawing

Figure 4.4: Clump weight comparison with design drawing, seen from above

The added mass coefficient decided on was 1.0, as the clump weight will be lifted over the sea bed before impact for the higher free spans. A sensitivity study was performed to see whether this decision had a significant impact on the pull over force, and results showed that the added mass coefficient

had a negligible effect on pull over forces. Therefore it was decided to run all simulations with clump weight added mass coefficient equal to 1.0.

The clump weight is restrained from translation in lateral direction along the pipe, and from rotation in vertical and transversal direction. Introducing these restrictions ensured that the clump weight will collide with the pipeline at the pipe midspan each time.

The clump weight input data used in the simulations is shown in table 4.2.

Description	**Symbol**	**Value**	**Unit**
Roller diameter	D_r	0.76	m
Roller length	l_r	1.55	m
Dry mass	m_d	6100	kg
Added mass coefficient	C_a	1.0	-
Submerged mass	m_s	5316	kg

Table 4.2: Clump weight data

4.1.3 Warp line

The warp line was modelled in one lower and one upper part. The lower part could come in contact with the pipeline, and consist of many linear pipe elements. The element mesh size is reduced towards the warp line bracket, to maintain a consistent contact interface. In the 350 mm and 530 mm case the lower part is 2.05 m long with 130 elements. In the 840 mm case the lower part had to be longer due to the large pipe diameter to avoid interaction between the upper part of the warp line and the pipeline. In the 840 mm case the lower warp line is 2.55 m, with 190 elements. The total warp line length is equal in all cases. The lower warp line bending stiffness is very low to allow warp line bending during interaction.

As recommended by Kristian Maalø, the lower warp line was modelled without added mass and drag force to avoid unnatural oscillations occurring. However, the pipe elements found in the lower warp line had to be given mass. Thus, the submerged weight is equal to the weight in air. Maalø has verified that the simplified warp line properties were of less importance for the pull over results [12].

Input data for the lower warp line can be seen in table 4.3.

The upper warp line consist of one cable element, without mass and drag,

Description	Symbol	Value	Unit
Length	l_{lw}	2.05	m
Axial stiffness	EA	26.8	MN
Bending stiffness	EI	1.5	kNm^2
Added mass coefficient	C_a	0.0	-
Drag coefficient	C_d	0.0	-
Dry mass	m_d	4.0	kg/m
Submerged mass	m_s	4.0	kg/m

Table 4.3: Lower warp line data

and will work as a linear spring. In the 350 mm and 530 mm case, the upper warp line is 892.1 m. For the 840 mm case, the upper warp line is 891.6 m. The stiffness of the warp line is 30 kN, found from the experimental model tests [16]. Input data for the upper warp line can be seen in table 4.4.

Description	Symbol	Value	Unit
Length	l_{uw}	892.1	m
Axial stiffness	EA	26.8	MN
Added mass coefficient	C_a	0.0	-
Drag coefficient	C_d	0.0	-
Structural dry mass	m_d	0.0	kg/m
Submerged mass	m_s	0.0	kg/m

Table 4.4: Upper warp line data

4.1.4 Sweep lines

The sweep lines are modelled with cable elements, one element for each sweep line. The length is 40 m, found from the experimental model test [16]. Sweep line input data can be seen in table 4.5. [12]

Description	Symbol	Value	Unit
Length	l_s	40	m
Axial stiffness	EA	40	MN
Added mass coefficient	C_a	1.0	-
Drag coefficient	C_d	1.0	-
Structural dry mass	m_d	0.0	kg/m
Submerged mass	m_s	0.0	N/m

Table 4.5: Sweep line data

4.2 Pipeline data

two different pipeline models were created. One with the same configuration as in the model test, and one real case pipeline model. The real case model is 1000 m long and has realistic pipe material properties. The experimental test model is 25 m and made nearly totally rigid to be like the pipeline in the model test.

4.2.1 Experimental test model

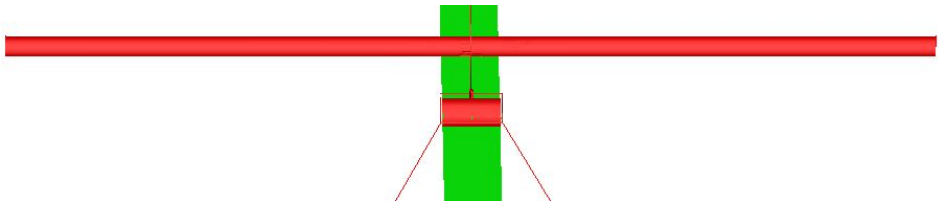

Figure 4.5: Experimental test model seen from above

Experimental test model simulations were performed with the same input values as used in the model test. The objective is to reproduce model tests numerically and analyse the response from clump weight over-trawling pipelines. Results are wanted to differentiate between the importance of effects from different parameters as free span height, pipeline diameter, flexibility in pipeline and clump weight geometry.

Free span heights were chosen based on available model test results. Three different free span heights were considered enough to find some relations between free span heights and pull over forces. Pipeline diameter was chosen

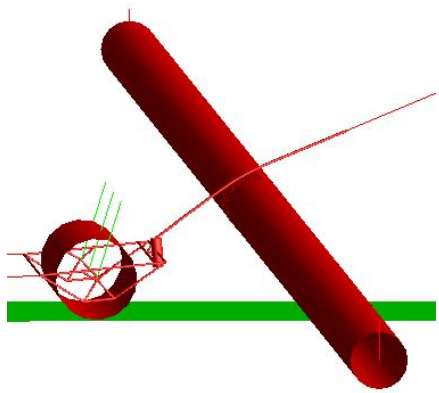

Figure 4.6: Experimental test model seen from the side

to be the same as in the experimental model tests, 350 mm, 530 mm and 840 mm pipeline diameter.

The pipeline is modelled with both flexible and fixed pipe end conditions. The flexible ends are represented with springs allowing the pipeline to move in translational direction, having the same stiffness as used in the model test. In the fixed case end springs are removed and pipe ends fixed against translation and rotation. A spring pre-tension was necessary to obtain a reasonable pipeline displacement, compared to model test results. It is also confirmed that some pre-tension was present during the model test [12]. This pre-tension is applied in the spring stiffness curve, see figure 4.7 for the 350 mm pipeline diameter stiffness case. Pipe damping was also applied in the spring element.

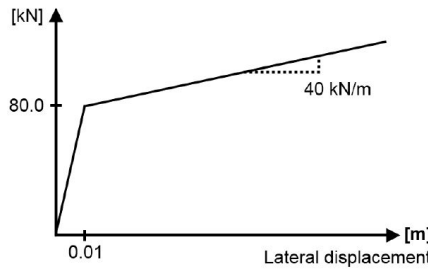

Figure 4.7: Spring stiffness curve [12]

The pipeline consists of 100 pipe elements, each with a element size of 0.25 m. Experimental test model input data can be found in table 4.6, 4.7 and 4.8 for 350 mm, 530 mm and 840 mm pipeline diameters respectively.

Description	Symbol	Value	Unit
Length	L	25	m
Pipe diameter	OD	350	mm
Pipe thickness	t_h	20	mm
Dry mass	m_d	405.9	kg/m
Submerged mass	m_s	307.3	kg/m
Added mass coefficient	C_a	1.0	-
Drag coefficient	C_d	1.0	-
Total pipe end stiffness	k_s	80	kN/m
Pipe end pretension	F_s	80	kN
Total pipe end damping	c_s	10	kN/m/s

Table 4.6: Pipeline data experimental test model, 350 mm

Description	Symbol	Value	Unit
Length	L	25	m
Pipe diameter	OD	530	mm
Pipe thickness	t_h	20	mm
Dry mass	m_d	725.7	kg/m
Submerged mass	m_s	499.6	kg/m
Added mass coefficient	C_a	1.0	-
Drag coefficient	C_d	1.0	-
Total pipe end stiffness	k_s	80	kN/m
Pipe end pretension	F_s	80	kN
Total pipe end damping	c_s	20	kN/m/s

Table 4.7: Pipeline data experimental test model, 530 mm

Description	Symbol	Value	Unit
Length	L	25	m
Pipe diameter	OD	840	mm
Pipe thickness	t_h	20	mm
Dry mass	m_d	2078.7	kg/m
Submerged mass	m_s	1510.7	kg/m
Added mass coefficient	C_a	1.0	-
Drag coefficient	C_d	1.0	-
Total pipe end stiffness	k_s	200	kN/m
Pipe end pretension	F_s	80	kN
Total pipe end damping	c_s	70	kN/m/s

Table 4.8: Pipeline data experimental test model, 840 mm

4.2.2 Full scale pipeline model

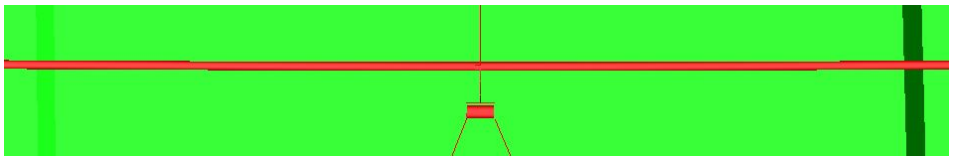

Figure 4.8: Full scale pipeline model seen from above

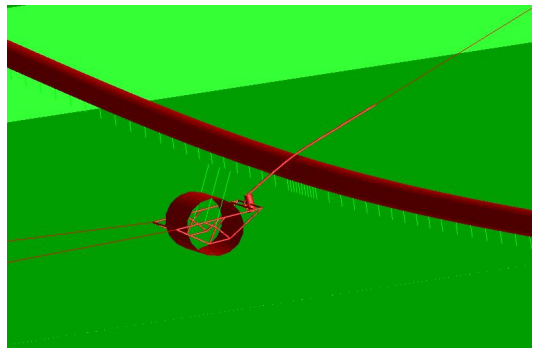

Figure 4.9: Full scale pipeline model seen from the side

The full scale pipeline data was presented by Reinertsen AS, and modified to be comparable with the experimental test model simulations. The diameters were chosen to be the same as in the experimental test model, but in this model it included coating. In addition, the wall thickness is a bit thicker in the full scale model. The pipeline is 1000 m long, and has a free span width of 50 m at the middle of the pipeline. The element size is 14 m at the pipeline ends but gradually reduced approaching mid point of the pipeline, where the element size is 0.2 m. A total of 270 linear pipe elements are used. The pipeline ends are fixed, assuming rock dumping, so that the ends does not displace during interaction. The full scale pipeline model is more physically precise, as it has realistic material properties and thus transversal and vertical flexibility. The pipeline is modelled with linear material properties and in empty condition, meaning no internal pressure or temperature. This is done to simplify the model and reduce computational time. The global clump weight pipeline response is emphasised, not focusing on local pipeline integrity.

When varying free span height, the pipeline and belonging sea bed are moved vertically while the sea bottom and trawling equipment are kept constant.

The sea bed is totally flat, except at change in free span, and soil properties are realistic. The soil properties are provided by Reinertsen AS, and are the same properties as Maalø used in his master thesis [12].

The full scale pipeline data can be seen in table 4.9 and 4.10 for 350 mm and 530 mm diameter pipeline respectively.

Description	**Symbol**	**Value**	**Unit**
Length	L	1000	m
Free span length	l_{fs}	50	m
Pipe steel diameter	D_s	344	mm
Pipe outer diameter	OD	350	mm
Pipe steel thickness	t_h	23	mm
Coating thickness	t_c	3	mm
Dry mass	m_d	185.2	kg/m
Submerged mass	m_s	86.59	kg/m
Added mass coefficient at seabed	$C_{a,sb}$	2.29	-
Added mass coefficient at free span	$C_{a,fs}$	1.0	-
Drag coefficient	C_d	1.0	-
Youngs modulus	E	207	GPa
Shear modulus	G	80	GPa
Axial stiffness	EA	4890	MN
Bending stiffness	EI	65.7	MNm^2

Table 4.9: Full scale pipeline data, 350 mm diameter pipeline

Description	Symbol	Value	Unit
Length	L	1000	m
Free span length	l_{fs}	50	m
Pipe steel diameter	D_s	520	mm
Pipe outer diameter	OD	530	mm
Pipe steel thickness	t_h	25	mm
Coating thickness	t_c	5	mm
Dry mass	m_d	313.08	kg/m
Submerged mass	m_s	86.95	kg/m
Added mass coefficient at seabed	$C_{a,sb}$	2.29	-
Added mass coefficient at free span	$C_{a,fs}$	1.0	-
Drag coefficient	C_d	1.0	-
Youngs modulus	E	207	GPa
Shear modulus	G	80	GPa
Axial stiffness	EA	8200	MN
Bending stiffness	EI	260	MNm^2

Table 4.10: Full scale pipeline data, 530 mm diameter pipeline

4.3 DNV-RP-F111 Point load model

A point load model was created to find the design load in each of the previous cases, enabling a comparison between pipeline design and simulations. For each case, a point load model was created with identical pipeline properties, but the clump weight and trawl equipment was replaced by the point load.

The point load was established using equations from DNV-RP-F111, where the maximum horizontal force (equation 2.1) and pull over duration (equation 2.5) can be found [5]. The values were implemented in SIMLA as a point load, with the force time history as seen in figure 4.10. The model was analysed in SIMLA several times for each case as an iteration process, until the displacement used in the pull over time equation agreed with the actual displacement in SIMLA.

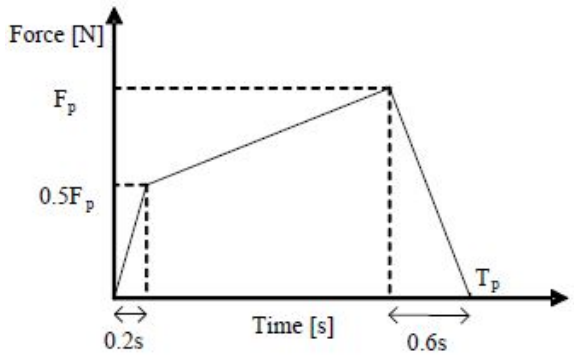

Figure 4.10: Clump weight pull over force time history from DNV [5]

4.4 Contact interaction

4.4.1 Clump weight pipeline contact

Two sets of contact groups were used in the models. One ensuring contact between the lower warp line and pipeline, and another ensuring contact between the warp line bracket and pipeline. Applying contact elements on the clump weight frame and roller was considered as well. After advice from Maalø who tested this in his master thesis, a decision was made not to expand the contact area. This was justified by the shortening of modelling and simulation time. Also, results from Maalø states that an expanded contact area had little or no influence on the pull over results, except for a high transient after maximum pull over [12].

For each group of structural elements in the model where contact is wanted, a contact group is established. The contact group consist of slave elements and their belonging master elements. Slave elements are a set of structural elements, while the master elements are a set of contact elements. In the master thesis, slave elements are structural pipe elements. During an interaction the contact elements search, locate and establish contact with the slave element. The contact element is searching for slave elements in each time increment. If a slave element is within the search area of a master element, the distance between outer slave element and master element is calculated. If the distance is negative, the slave element is in contact with the master element and forces are transferred. In SIMLA there is a variety of different contact elements available. In the master thesis cont164 roller elements are used for all cases. [20] [19]

Material stiffness curves in axial, normal and circumferential directions are used to describe the contact-interaction. Material curves are applied based on the penalty method [20]. A force-indentation curve is used to describe the normal stiffness in the contact elements. This curve is shown in figure 4.11 and is found from experiment where a 25 mm steel rod perpendicular to a pipe were forced into the pipe coating. The pipeline had a diameter of 280.5 mm and the coating was 18 mm thick. [21], [12]

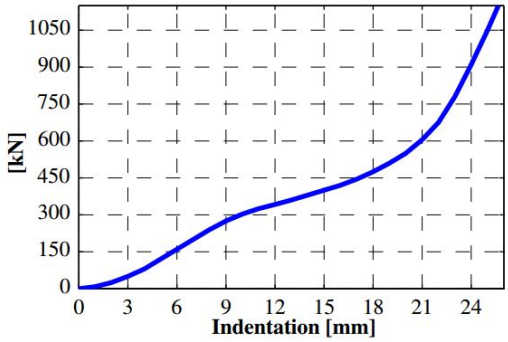

Figure 4.11: Force-indentation in pipe wall [21]

The axial and circumferential interaction curves can be seen in figure 4.12. The friction force is applied by a Coulomb friction model, scaling the curve with normal contact force and a specified friction coefficient [12]. The results seemed to be independent of the applied friction coefficient, when varied between 0.0 and 2.0. Therefore, simulations are assumed performed without friction in both axial and circumferential direction.

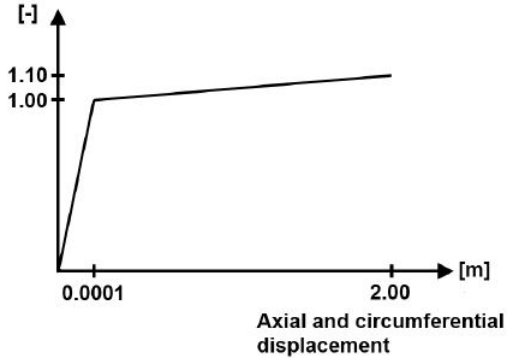

Figure 4.12: Axial and circumferential stiffness curve for contact elements [12]

Pipeline warp line contact

Warp line pipeline contact group was established with only one master element. This master element was connected to the mid-node in the pipeline, having the same diameter as the pipeline diameter. The lower warp line consist of 130 (190 in the 840 mm pipeline diameter case) linear pipe elements representing the slave element group, see figure 4.13. The slave elements are coloured green, and the single master element is coloured red.

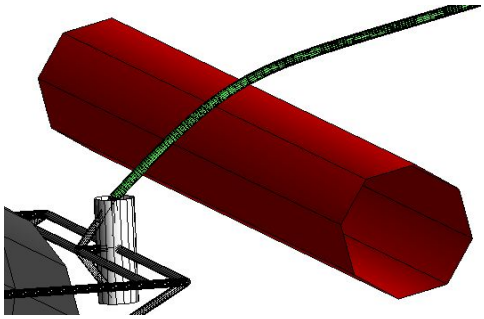

Figure 4.13: Contact group: pipeline and warp line

Pipeline warp line bracket contact

The pipeline warp line bracket contact group was established with several master elements. The master elements are small circular rollers defining the outer pipeline. The slave element is a single linear pipe element representing the warp line bracket. This is shown in figure 4.14, where the slave element is coloured green, and the master elements coloured red.

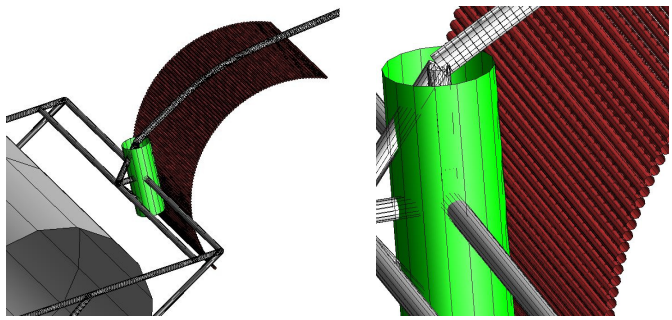

(a) Seen from the side (b) Close up

Figure 4.14: Contact group: pipeline and warp line bracket

4.4.2 Seabed contact

Seabed interaction data is not altered from what was used in Maaløs master thesis [12]. The seabed is entirely flat along the entire pipeline and clump weight road stretch. The seabed is divided in a grid, and each square can be assigned different soil properties. Soil properties are identical in the different models, though the seabed extension differs. In the experimental test model the sea bed area is only a strip along the clump weight roller road. In the full scale model the sea bed is extended all the way to the pipe ends, see figure 4.15.

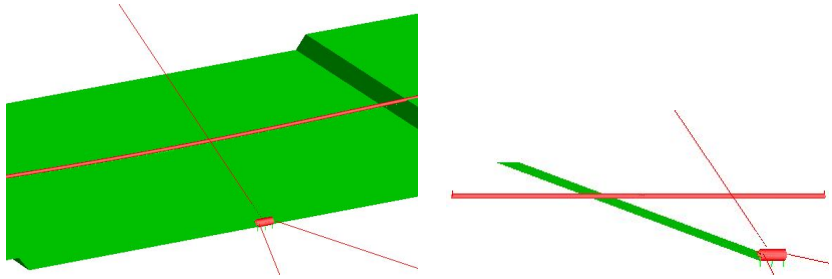

(a) Full scale model (b) Experimental test model

Figure 4.15: Extension of seabed

The seabed contact is modelled with special purpose seabed contact elements where interaction is obtained applying springs in each node where contact is wanted, i.e. between pipeline and seabed, and clump weight and seabed. A friction force is applied in both transversal and axial

direction. The friction characteristics are decided by use of interaction curves, defining an unit friction force per meter displacement. In the master thesis, Coulomb friction is applied for each length unit in contact with the seabed. In SIMLA, a scaling factor is used for the curves and in the master thesis a scaling factor equal 1.0 is used for all cases. [12]

Pipeline seabed contact

The seabed contact elements are, for the full scale model, included in each of the pipeline nodes. Friction is applied in both transversal and axial direction, illustrated in figure 4.16 [12]. The interaction coefficients was provided by Reinertsen AS. These are estimates for a 12" pipeline in soft clay. An additional interaction curve is applied in transversal direction, and only activated for penetrations larger than 0.07 m. This additional curve is needed to determine pipeline breakout resistance. Vertical soil resistance is chosen such that the pipeline is allowed to penetrate the seabed with 1/5 of the outer diameter at the free span ends. The free span is created by lowering the seabed between two nodes, at the requested depth. [12]

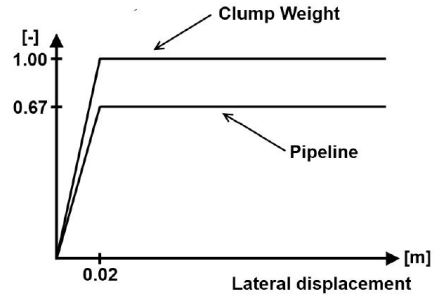

(a) Transversal seabed interaction curve

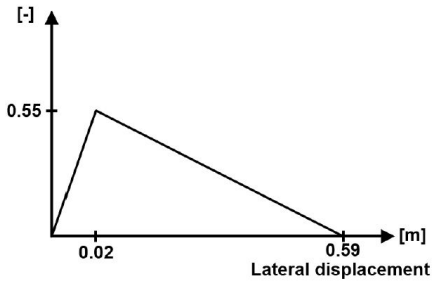

(b) Additional seabed interaction curve

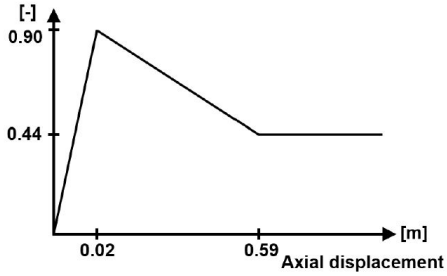

(c) Axial seabed interaction curve

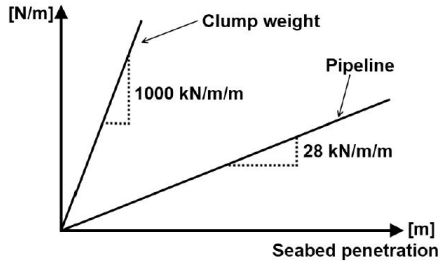

(d) Vertical seabed interaction curve

Figure 4.16: Seabed contact interaction curves [12]

Clump weight seabed contact

The clump weight seabed contact is defined in three nodes along the clump weight roller. Soil properties related to the clump weight path is different compared to rest of the seabed. Vertical soil resistance is higher, helping the clump weight avoid sinking into the sediments. Additionally, the friction coefficient in transversal direction is set to equal 1.0, making the clump weight able to roll at the seabed rather than gliding. Lastly the clump weight is retained from translation in axial direction. The clump weight seabed interaction curves is shown in figure 4.16, where the points of interest are indexed a) and d). [12]

4.4.3 Contact damping

When estimating contact damping, a local eigenfrequency damping is used [12]. Damping is applied across all contact points, that is clump weight and pipeline, clump weight and seabed and pipeline and seabed. The damping coefficient is estimated considering local mass, added mass and the applied normal contact stiffness. The following formula is used:

$$C = 2\lambda\sqrt{(m + m_a)k_c} \tag{4.1}$$

C is the damping coefficient, λ the damping ratio and k_c the normal contact stiffness. m is the structural mass and m_a the added mass.

4.5 Structural damping and added mass

Structural damping

Rayleigh damping is used to describe the structural damping. The damping force is defined proportional to the mass matrix, $\mathbf{M}$, and stiffness matrix $\mathbf{K}$. See equation 4.2.

$$\mathbf{C} = \alpha_\mathbf{1}\mathbf{M} + \alpha_\mathbf{2}\mathbf{K} \tag{4.2}$$

α_1 and α_2 are constants used to define the damping magnitude. The term proportional with the mass matrix damp out low frequencies, while the term

proportional with the stiffness matrix damp out high frequencies [7]. In the simulations some stiffness proportional damping is applied, to damp out high frequencies. No mass proportional damping is applied, hence α_1 equal 0.

To approximate the stiffness proportional damping magnitude, Maalø executed a sensitivity study where he varied α_2 between 0.02 and 1.16. The preferred α_2 after this study was an α_2 equal 0.095. The same value has been used throughout this master thesis. [12]

Added mass

SIMLA applies added mass using the following formula:

$$m_a = C_a \pi \rho r^2 l \tag{4.3}$$

m_a is the added mass and C_a the added mass coefficient. Only the added mass coefficient is applied to the input file. In an infinite fluid, the added mass for a cylinder is equal to the mass of the displaced water, hence C_a equal 1.0 [6]. When a cylinder moves towards a wall, the added mass coefficient rises and when the cylinder is digging into the wall or seabed, C_a is equal to 2.29 [6]. The recommended practice for interference between trawl gear and pipelines state that an added mass coefficient of 1.83 should be used for the clump weight. This factor is based on the added mass coefficient for a cylinder digging into a wall, with a reduction factor of 0.8 due to finite cylinder length [5]. However, in the recommended practise for free spanning pipelines, an added mass coefficient of approximately 1.0 is recommended for all free spanning pipeline cases [4]. As the clump weight is lifted over the sea bed before hitting the pipeline, it could be argued that the clump weight as well could have an added mass coefficient equal to the pipeline added mass. Therefore, the decision was made to apply clump weight added mass coefficient equal to 1.0 in all cases. This is discussed further in chapter 5.2.4.

4.6 Analysis procedure

The analysis is started by placing the clump weight 20 m from the pipeline. The first two seconds are a statical analysis where the clump weight is

retained from rotation. During the first second all statical loads, like gravity and outer pressure, are applied. After one second the towing node start to accelerate, and the warp line is tensioned. After two seconds the analysis is stopped and restarted as a dynamic analysis. This is done manually in the input file in FlexEdit. Simultaneously, restraints on clump weight rolling are removed. The towing node is accelerated gradually until the desired velocity of 1.95 m/s is reached, after about 10 seconds. Constant drag resistance and back tension from trawl nets are reached after 15 seconds. It is at this time 1-2 seconds before clump weight pipeline impact.

In the full scale model, the free span height was adjusted and calculated after the first two seconds, since the pipeline would bend due to the free span, reducing the free span height. The warp line is gliding over the pipeline before impact. As a consequence the pipeline in the full scale model is being pushed down further by the warp line before clump weight impact, reducing the free span height by a slight amount. This reduction is not taken into account in the analyses. The analysis is stopped after 25 seconds in the experimental test model, and after 33 seconds for the full scale model. By this time, the clump weight is released from the pipeline and pull over results completed.

The convergence criteria had a tolerance of 10^{-5} for each equilibrium iteration and take care of the unbalanced damping, inertia and internal forces [19]. Time steps were varied for different parts of the simulation. During the first twelve seconds of towing node acceleration, a time step of 10^{-2} was necessary to reach a smooth transition and a satisfactory amount of equilibrium iterations. During trawl gear pipeline interaction a time step of 10^{-3} was necessary. The CPU time used was approximately 10-20 minutes for the experimental test model, and 25-45 minutes for the full scale model when using an average consumer grade laptop with an Intel Core i5 1.7 GHz ULV CPU from 2012.

4.7 Post processing and sampling of results

The clump weight hits the pipeline at the pipeline mid-node. Pipeline shear forces are sampled at two nodes, one in each of the two elements adjacent to the mid-node. The nodal forces are summarized, and total pull over force is obtained. The reason for sampling forces as shear forces, and not as direct contact forces between master and slave elements, are due to the number of master and slave elements in the model. It would be very time consuming

and not very practical.

The nodes are determined by a local coordinate system, but during interaction pipeline elements will rotate and deform according to a global coordinate system. This leads to a source of error, where some of the forces will be absorbed as an axial contribution. Thus, the shear force will be slightly lower than the actual horizontal pull over force. This is not taken into account in the master thesis, as axial forces are presumed to be small. Also, drag forces and inertia forces along the element will reduce the shear force, but as the element size is small around pipeline mid-node, the effect will be very small and is ignored in the master thesis. Thus, what is referred to as horizontal pull over force from simulations, are actually a transversal shear force in the pipeline.

When analyses in SIMLA are finished, shear forces are loaded into MATLAB where accompanying nodal forces are summarized and presented as graphs of interest, i.e. normalized graphs comparing simulation force with design load and model test pull over force.

Model test results were made available in this master thesis for verification purposes. Model test plots in chapter 5 are digitalized from the model test report and additional result files provided by Reinertsen AS [16]. All model test plots are low pass filtered due to large vibrations in the pipe line during and after impact [16]. Simulation results are not low pass filtered in the graphs presented, but are low pass filtered when comparing maximum pull over force between simulation, model test and design load in table 5.2.

Chapter 5

Analysis results

Results gained during the master thesis are presented in this chapter. First results from experimental test model simulations in comparison with model test and design loads are presented for all three diameter cases. The experimental model test is described in chapter 2.4. In this chapter, simulation force is associated with horizontal pull over force from simulations when using SIMLA. The model test force is associated with horizontal pull over force from experimental model test results. The design load is associated with force found using the recommended practice, DNV-RP-F111, in each individual simulation.

Further, results from various sensitivity studies are presented, executed with experimental test model input. Finally, results from the full scale model are presented.

As discussed in chapter 4.7, pull over forces obtained from simulations are collected as shear forces in the pipeline at mid node of attack. Model test forces are collected from the end springs. When collecting forces from end springs, the forces can be influenced by damping or vibrations. It is presumed that the various locations for measuring forces are not significant for the results, even though it could explain some small variations.

As the model test report is restricted for publishing, all forces are made dimensionless by dividing the respective force on the belonging model test force. Unless stated otherwise, the normalized force is the normalized horizontal pull over force. A summary of all plots and the associated normalized force can be seen in appendix C, although values from model test results are not reported due to restrictions.

5.1 Experimental test model: Simulations in comparison with model tests

Simulations are varied in pipe diameter, pipe free span and end boundary conditions. In the master thesis simulations for 350 mm as well as 530 mm and 840 mm pipe diameter have been performed. Maalø performed a clump weight pull over interaction analysis with pipeline diameter 350 mm during his master thesis [12]. The 350 mm cases were simulated again in this master thesis as new version of SIMLA has been released, and certain changes in the input files have been made. A summary of the simulations with model test input can be seen in table 5.1.

Test no.	**Pipe diameter** mm	**Span height** m	**Pipe end condition**	**Tow velocity** m/s	**Total Spring stiffness** kN/m	**Damping** kN/(m/s)	**Warp stiffness** kN/m
3340	840	0.75	Flex	1.95	200	70	30
3250	840	0.5	Flex	1.95	200	70	30
3160	840	0.25	Flex	1.95	200	70	30
3360	840	0.75	Fixed	1.95	Fixed	Fixed	30
3270	840	0.5	Fixed	1.95	Fixed	Fixed	30
3180	840	0.25	Fixed	1.95	Fixed	Fixed	30
3310	530	0.75	Flex	1.95	80	20	30
3220	530	0.5	Flex	1.95	80	20	30
3130	530	0.25	Flex	1.95	80	20	30
3330	530	0.75	Fixed	1.95	Fixed	Fixed	30
3240	530	0.5	Fixed	1.95	Fixed	Fixed	30
3150	530	0.25	Fixed	1.95	Fixed	Fixed	30
3281	350	0.75	Flex	1.95	80	10	30
3190	350	0.5	Flex	1.95	80	10	30
3100	350	0.25	Flex	1.95	80	10	30
3300	350	0.75	Fixed	1.95	Fixed	Fixed	30
3210	350	0.5	Fixed	1.95	Fixed	Fixed	30
3120	350	0.25	Fixed	1.95	Fixed	Fixed	30

Table 5.1: Experimental test model simulation configuration

The general presentation of results are divided in pipe diameter and free span height. Sensitivity studies are presented at last.

5.1.1 840 mm pipeline diameter

The first case is 840 mm diameter pipeline with 0.75 m free span height. Horizontal pull over force is shown in figure 5.1, for both flexible and fixed pipe end conditions. In the figures "SIMLA" represent the simulated pull over force, "Test" represents pull over force from model tests, and "DNV" represent the design load. The horizontal pull over force from simulation is higher than the force from model test and design load. This is somewhat unexpected, as one would expect the design load to be higher than simulation pull over force for all cases. However, the design load is considerably higher than the model test force.

It is also worth noticing that the difference in pull over forces between flexible and fixed pipe end conditions are minor.

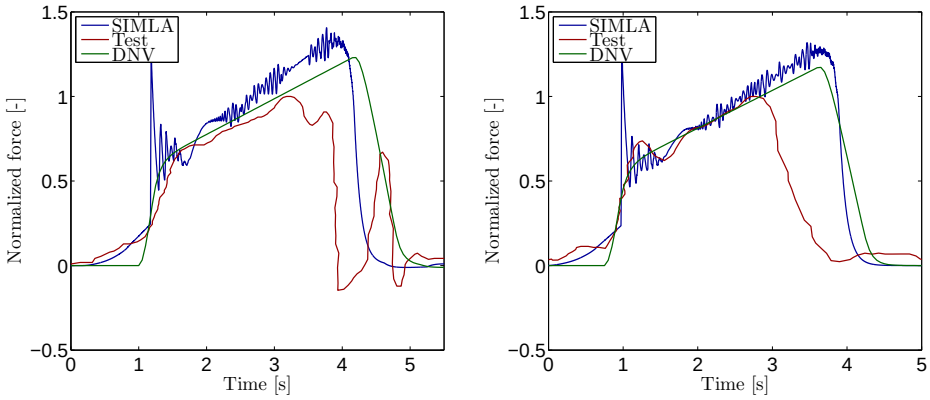

(a) Flexible condition (b) Fixed condition

Figure 5.1: 840 mm pipeline diameter, 0.75 m free span

Results from 840 mm, 0.5 m free span is shown in figure 5.2. Both a) and b) show similar tendencies, as simulation pull over forces are slightly higher than design loads, while model test pull over forces are somewhat smaller.

Results from 840 mm, 0.25 m free span is presented in figure 5.3. In the fixed case there is a distinct difference from previous cases, where the model test pull over force is considerably higher than the pull over force from both simulation and design load. The simulation force is slightly higher than the design load.

One possible explanation for the high model test force in the 0.25 m fixed condition is given in model test videos. When comparing the videos from

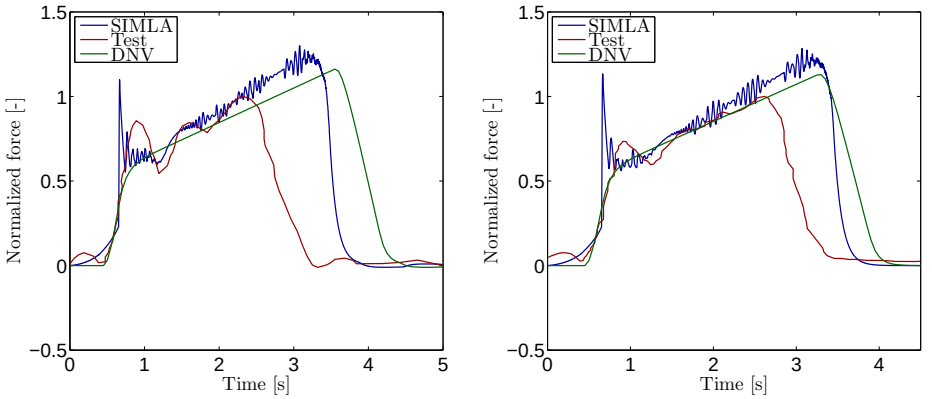

(a) Flexible condition (b) Fixed condition

Figure 5.2: 840 mm pipeline diamter, 0.5 m free span

various model test runs, a variation in clump weight wobbling is observed. In test number 3270 (corresponding with 840 mm, 0.5 m free span, fixed condition) it is possible to see wobbling in the clump weight, before and especially after impact. While for test number 3180 (corresponding to 840 mm, 0.25 m free span, fixed condition) it seems like there is no wobbling at all. Because of this observation a sensitivity study was performed investigating wobbling, finding a distinct relation between increased wobbling and decreased pull over force. The sensitivity study is presented in section 5.2.1, and a screen shot from one of the simulated wobbling cases can be seen in figure 5.4.

The clump weight is pulled over the pipeline due to pull force in the warp line. When the clump weight hit the pipeline while wobbling, it will hit the pipeline with an initial tilt relative to the horizontal direction. The tilt could create a momentum causing the clump weight to be pulled over the pipeline more easily, resulting in shorter pull over time and thus lower pull over force [5] The wobbling effect could explain the long pull over time and high force in the 0.25 m fixed case, as no wobbling was observed in this model test video.

The peaks at impact for SIMLA-plots are likely due to transients occurring, and could be a numerical effect. All maximum values are collected at end peak of pull over time.

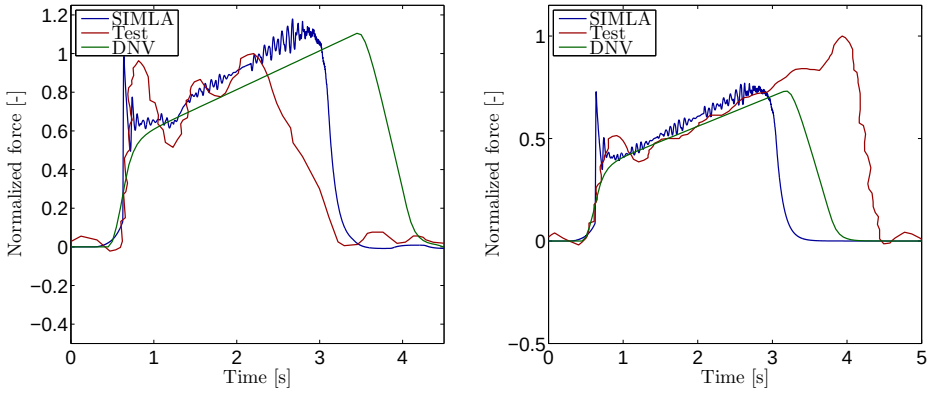

(a) Flexible condition (b) Fixed condition

Figure 5.3: 840 mm pipeline diameter, 0.25 m free span

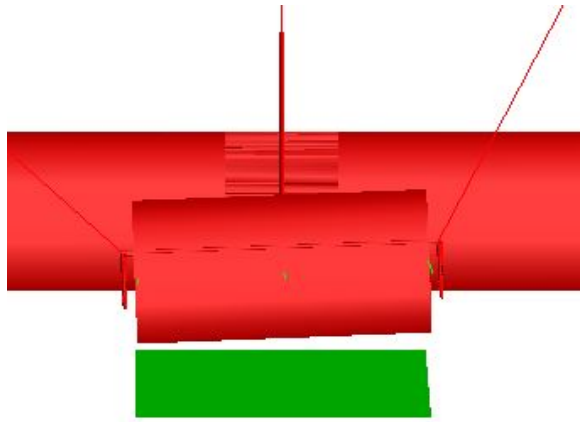

Figure 5.4: Clump weight tilt, 840 mm, 0.5 m free span, fixed condition

5.1.2 530 mm pipeline diameter

Results from 530 mm diameter cases can be seen in figure 5.5, 5.6 and 5.7. When comparing 0.75 m and 0.5 m free span they are quite similar. In the fixed cases, pull over plots from simulations and model tests are closely related in both pull over time and plot gradient progress. In 0.75 m and 0.5 m free span fixed cases, the different pull over peak forces are only distinguishable by some kN in each case.

The 0.25 m free span case stand out from the others in that pull over force

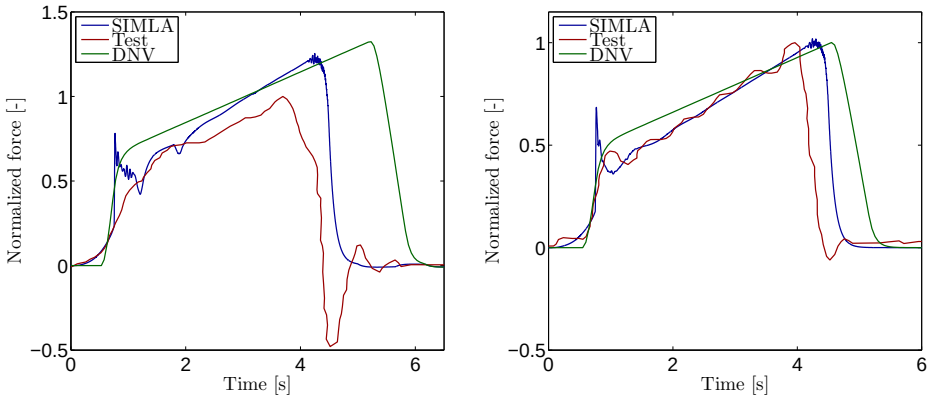

(a) Flexible condition (b) Fixed condition

Figure 5.5: 530 mm pipeline diameter, 0.75 m free span

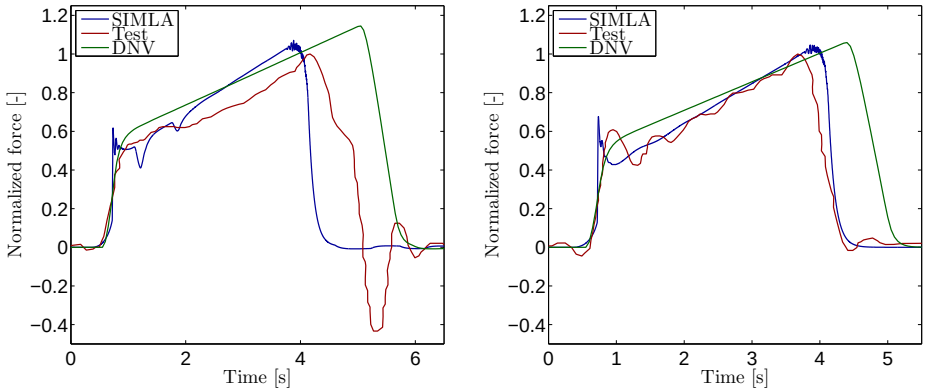

(a) Flexible condition (b) Fixed condition

Figure 5.6: 530 mm pipeline diameter, 0.5 m free span

and time from simulations are smaller than both model test pull over force and design load, both in flexible and fixed condition. The difference in pull over time for the 0.25 m case, compared to 0.5 m and 0.75 m cases, could be due to clump weight impact angle. Clump weights will hit pipelines less inclined with low free spans. The clump weight pipeline over-pulling distance will, in a radial sense, be shorter with low free spans than for a higher free span case, thus lead to lower pull over force. In higher free span cases the clump weight will hit the pipeline in a more inclined state, as it is lifted by the warp line before impact. This is illustrated in figure 5.8 (where

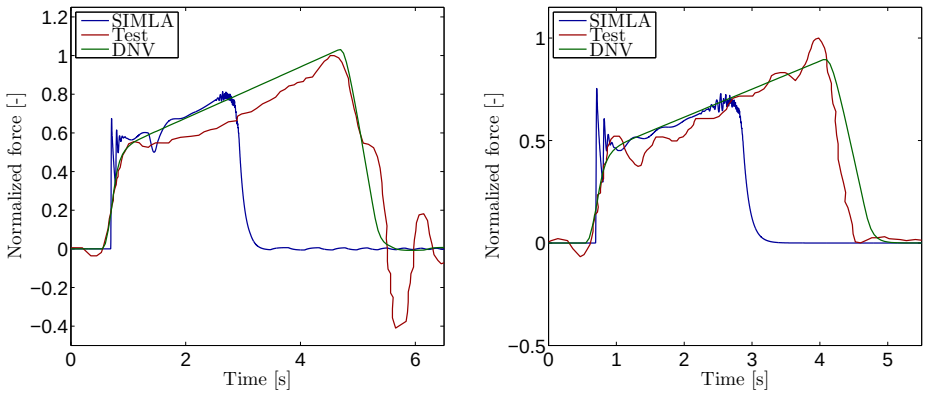

(a) Flexible condition (b) Fixed condition

Figure 5.7: 530 mm pipeline diameter, 0.25 m free span

the clump weight is more inclined at impact in the 0.5 m free span case than in the 0.25 m free span case).

When viewing low free span simulations in Xpost, yet another observation can be made where the clump weight is bounced back a short distance after first impact. This is the result of a high frequency impact where the warp line has yet to take hold of the pipeline, resulting in a shock in the pipeline clump weight system because of the sudden force interaction. In this case it will be more like a pure warp line bracket-pipeline interaction, where the warp line is contributing little to the force transferring occurrence. In higher free span cases, the warp line would already have interacted with the pipeline, making the first impact more steady avoiding a backstroke. In this case the warp line will contribute to the force transferring interaction due to pulling on the clump weight while interacting with the pipeline.

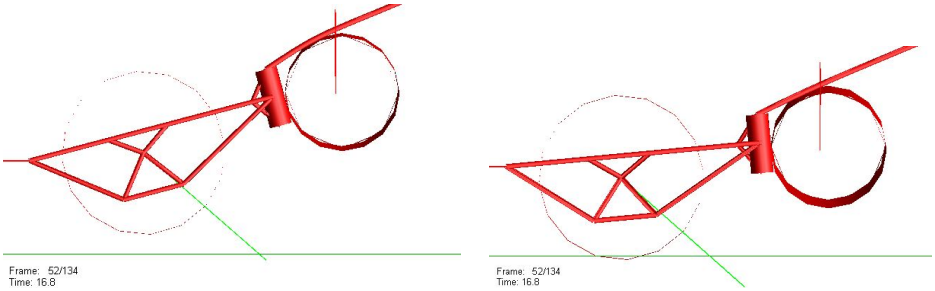

(a) 0.5 m free span (b) 0.25 m free span

Figure 5.8: Clump weight impact angle 530 mm pipeline diameter, flexible condition

5.1.3 350 mm pipeline diameter

The results resemble results seen in the 530 mm diameter cases. The design load is slightly higher than both pull over force from simulation and model test, for all cases. Results are shown in figure 5.9, 5.10 and 5.11.

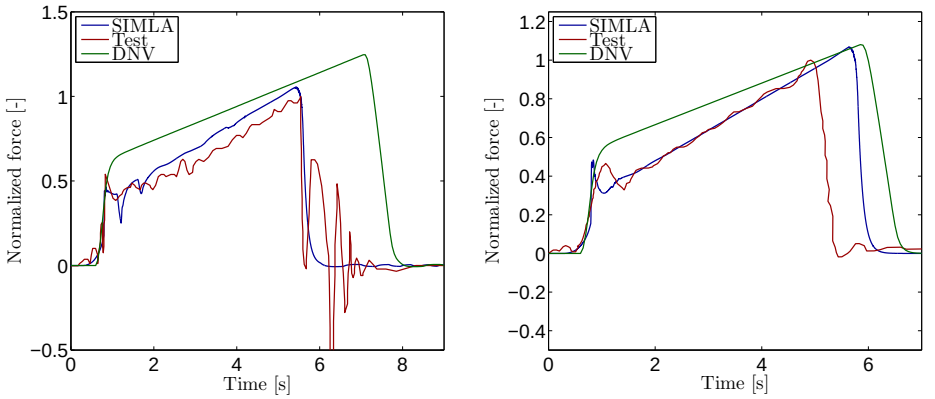

(a) Flexible condition (b) Fixed condition

Figure 5.9: 350 mm pipeline diameter, 0.75 m free span

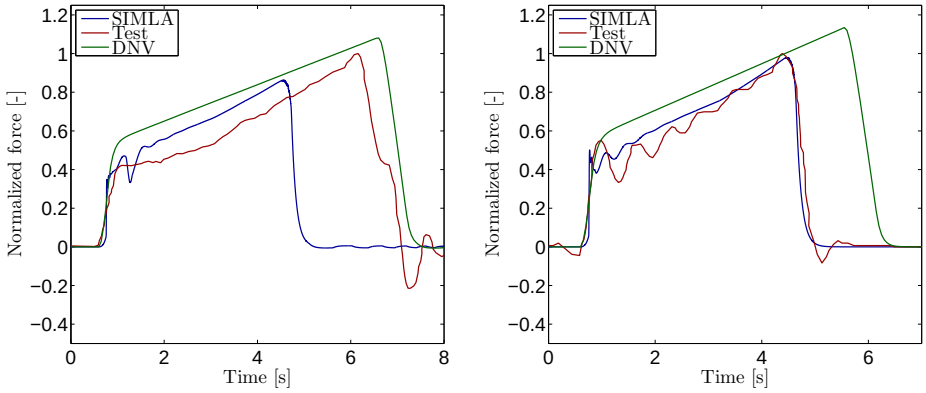

(a) Flexible condition (b) Fixed condition

Figure 5.10: 350 mm pipeline diameter, 0.5 m free span

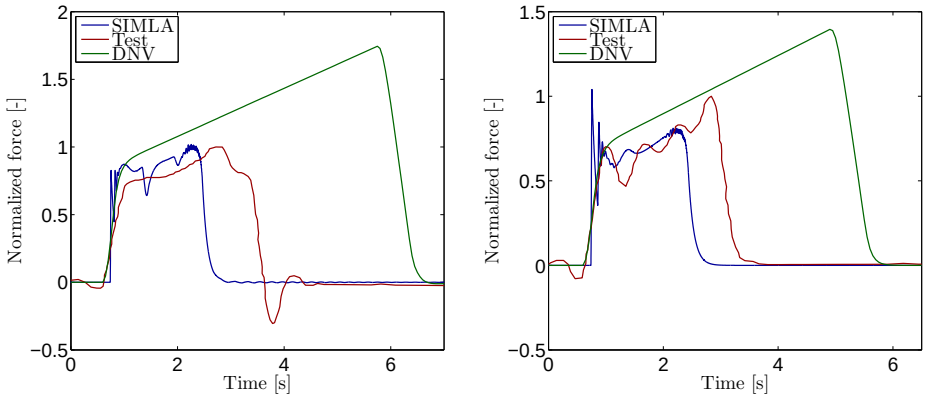

(a) Flexible condition (b) Fixed condition

Figure 5.11: 350 mm pipeline diameter, 0.25 m free span

5.1.4 Differences in results

Results from all model test cases is shown in table 5.2, and are expressed as a percentage deviation from experimental model test results. Simulation results in this calculation are smoothed using a low pass filer (filtered at 1.58 Hz) to be able to compare numbers directly with model test results. The choice of threshold is taken from the experimental model test report [16]. However, the table only includes maximum pull over force, and should be taken into consideration together with the plotted time histories.

		840 mm		530 mm		350 mm	
		SIMLA	DNV	SIMLA	DNV	SIMLA	DNV
		[%]		[%]		[%]	
Flexible	0.75 m	27,4	18,7	21,2	24,5	20,6	30,4
	0.5 m	21,6	13,9	7,6	12,7	-11,9	7,5
	0.25 m	13,4	9,5	-22,0	3,0	1,1	42,7
Fixed	0.75 m	24,1	14,7	3,5	0,1	9,4	7,4
	0.5 m	20,6	11,4	6,3	5,6	1,2	11,9
	0.25 m	-30,4	-36,8	-39,7	-11,8	-21,6	28,3

Table 5.2: Maximum pull over force percentage deviation from model tests, filtered simulation results

5.2 Sensitivity studies

Several sensitivity studies were performed to investigate certain parameters more thoroughly. Results from the different sensitivity studies can be found in the following sections.

5.2.1 Effect of clump weight wobbling

As some simulation results in the 840 mm diameter cases differed from the general norm, an in-depth study of these simulations was performed. Model test videos of the same cases were provided in corporation with Reinertsen AS and professor Svein Sævik. After watching model test videos a trend was noticed. Model test cases with a distinct higher horizontal pull over force than the general norm seemed to have no or very little clump weight wobbling at impact and after pull over. However, for the cases with short pull over time and lower pull over force, clump weight wobbling was to some extent detected at impact and after pull over. Simulated wobbling was initiated by modelling the sweep lines oblique to each other. This provided a tilted clump weight before impact and produced some simulated wobbling during and after impact.

Figure 5.12 show model test pull over force for case number 3270 (840 mm, 0.5 m free span, fixed condition) where a lot of clump weight wobbling was detected in the video. The same figure also includes pull over force from simulation with no wobbling and with some simulated wobbling. The simulated wobbling is represented by a reference angle between the two

sweep lines, were $\theta = 0°$ is a regular case with no wobbling and $\theta = 20°$ is the case with most simulated wobbling.

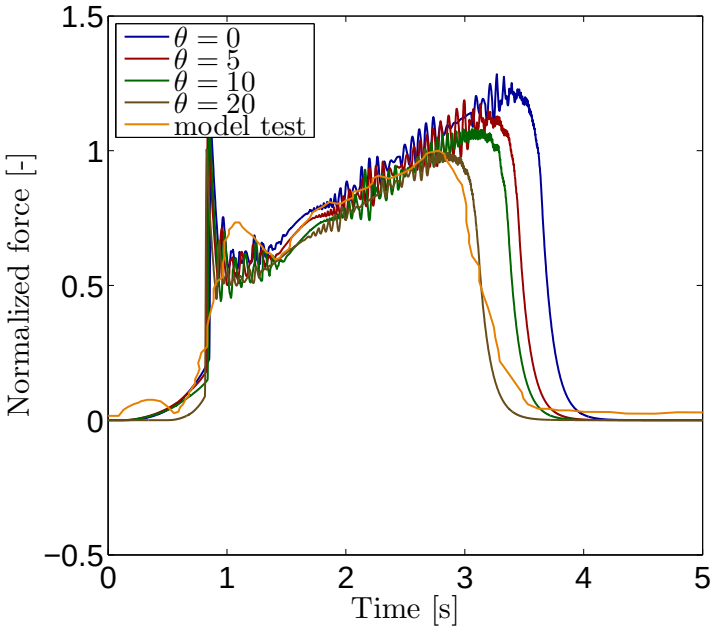

Figure 5.12: Pull over force with clump weight wobbling, 840 mm, 0.5 m free span, fixed condition

With wobbling present, the clump weight and warp line bracket could be tilted at pipeline impact and trigger a faster pull over history, reducing the pull over force. Wobbling could be connected to clump weight impact angle, as the warp line bracket could change with a different tilt angle.

Figure 5.12 indicate that it is an association between clump weight wobbling and pull over force, where the force might decrease with increased wobbling. As this effect also is visible from model test videos, this could suggest that some undocumented variations were present during execution of experimental model tests, which could have affected certain model test results.

5.2.2 Effect of increased pipeline diameter

Simulated horizontal pull over forces increase with decreasing pipe diameter, on the condition that the free span height is over a certain limit. All

simulation pull over forces follow the same force-time history gradient line, but the difference is the pull over time, thus maximum pull over force in each case. Results where the horizontal pull over force increase with decreasing pipe diameter are found for 0.75 m and 0.5 m free spans, and are presented in figure 5.13 and 5.14.

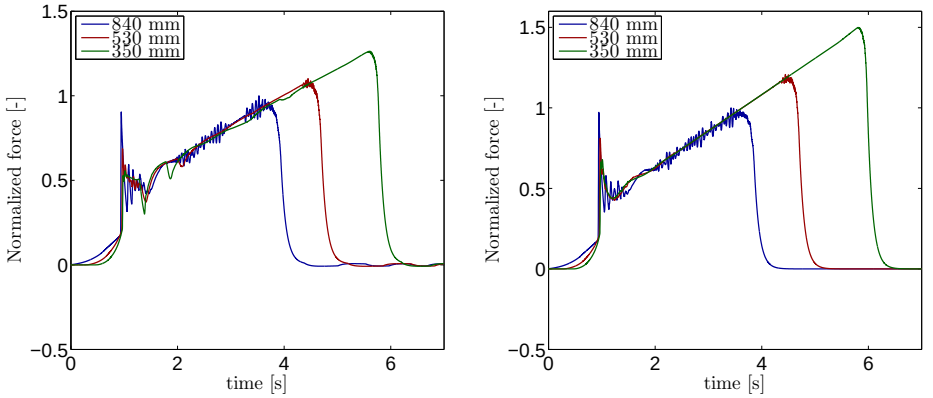

(a) Flexible condition (b) Fixed condition

Figure 5.13: Pull over force dependence on pipe diameter, 0.75 m free span

The difference in maximum pull over force for 0.75 m free span is -12.8% and -21% in the flexible case, and -19.5% and -33.3% in the fixed case, for 530 mm and 840 mm diameter cases respectively. Percentage results are based on the 350 mm 0.75 m free span flexible and fixed simulated case.

When having a small diameter pipeline and a high free span, the clump weight will be more inclined at time of interaction, than with a larger diameter pipeline. With an inclined clump weight, the warp line need to use more tension force to swing the clump weight over the pipeline in a pendulum-like movement. It could be noticed as the warp line bracket angle increase, the bracket experience a small hooking event, which results in a higher pull over force. However, with a large diameter pipeline, the warp line is able to pull the clump weight over the pipeline more directly, hence reducing pull over force and time. This effect is also mentioned in regard to the 530 mm cases, but then in connection with free span height. Screen shots from Xpost indicating this effect is seen in figure 5.15 and 5.16.

At initial impact, shown in figure 5.15, all diameters have somewhat similar clump weight impact angles, but the clump weight bracket hit the pipeline in different heights. However, as warp line tension increases and the clump

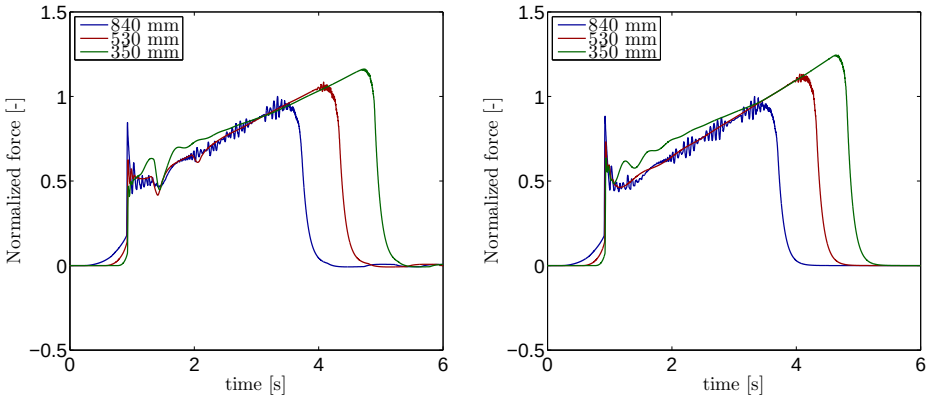

(a) Flexible condition (b) Fixed condition

Figure 5.14: Pull over force dependence on pipeline diameter, 0.5 m free span

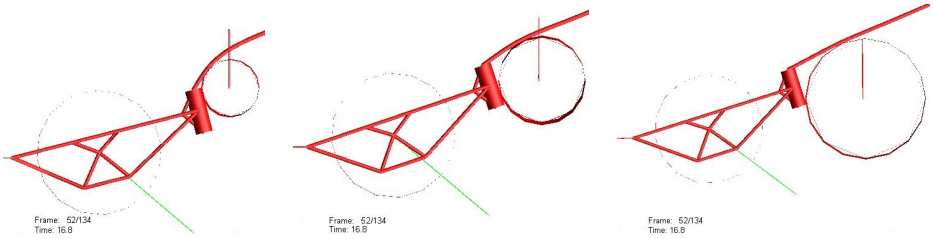

(a) 350 mm diameter (b) 530 mm diameter (c) 840 mm diameter

Figure 5.15: Screen shots from Xpost at initial impact, 0.75 m free span, at 16.8 sec

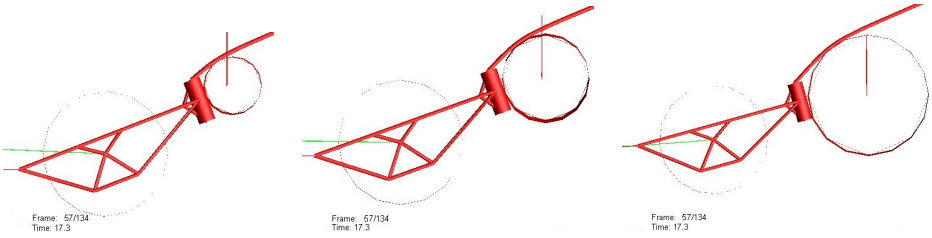

(a) 350 mm diameter (b) 530 mm diameter (c) 840 mm diameter

Figure 5.16: Screen shots from Xpost when the clump weight starts pulling on the pipeline, 0.75 m free span, at 17.3 sec

weight start to push on the pipeline (figure 5.16) it is obvious that the clump weight shifts its inclined angle according to the hypothesis, where the clump weight in figure 5.16 a) is more inclined than in c).

Result from 0.25 m free span is seen in figure 5.17.

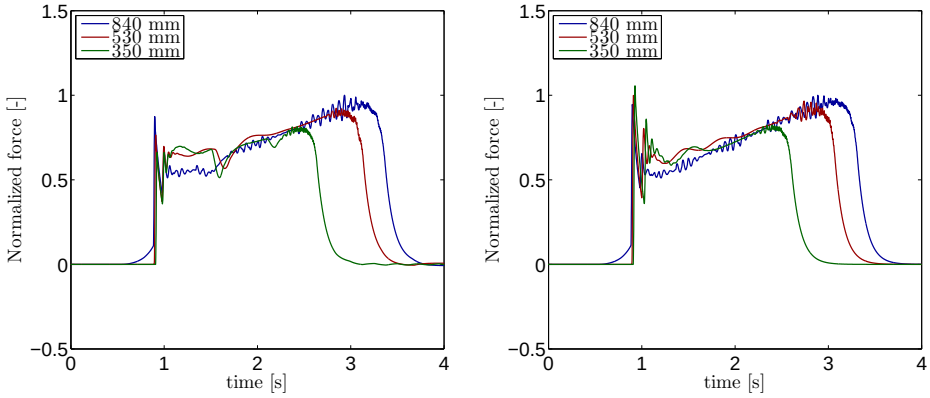

(a) Flexible condition (b) Fixed condition

Figure 5.17: Pull over force dependence on pipe diameter, 0.25 m free span

In the 0.25 m free span case the order is reversed, and the largest pipe diameter is experiencing the highest pull over force. This is further elaborated in section 5.2.3.

5.2.3 Effect of increased free span height

The effect of increased free span height was investigated by comparing maximum pull over force from simulations with maximum design loads, and comparing maximum design loads with maximum model test results, for all diameters and free spans. Design loads are included in each plot, being able to compare different plot results with each other. All values in this section are normalized with respect to maximum pull over force from simulation of 350 mm pipe diameter 0.75 m free span, flexible condition. The results are presented in figure 5.18 and 5.19.

For the simulation results, an increase in free span height lead to increased pull over force. Also, in both figure 5.18 a) and 5.19 a) it is observed that for 0.25 m free span, the largest pipe diameter gain the largest pull over force, and the 530 mm and 350 mm pipeline follows respectively. However, with increasing span height the order is reversed, and the smallest pipe diameter

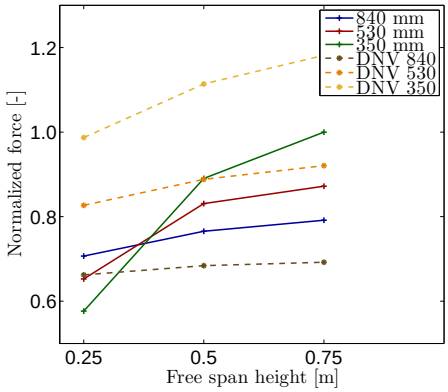

(a) Simulation force and design load

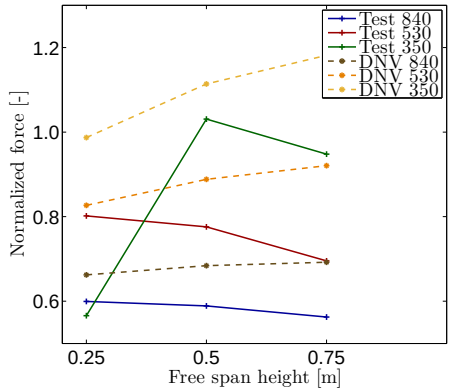

(b) Model test force and design load

Figure 5.18: Maximum pull over force dependence on free span height, flexible condition

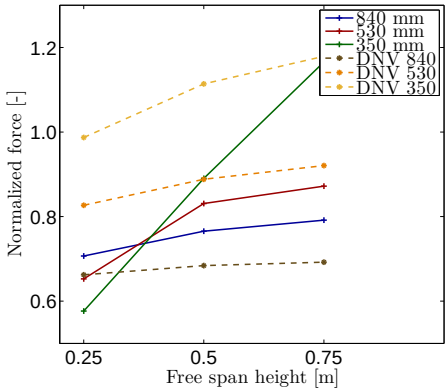

(a) Simulation force and design load

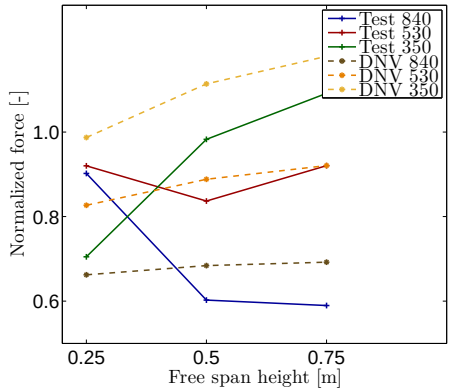

(b) Model test force and design load

Figure 5.19: Maximum pull over force dependence on free span height, fixed condition

obtain the largest pull over force, as pointed out and elaborated further in previous sections.

A definitive association is harder to prove with model test results, especially when including both flexible and fixed boundary conditions.

When comparing design loads with experimental model test results, one need to distinguish between flexible and fixed condition. In flexible condition the design load is higher than the model test force for all diameters and free

spans. In the development of the plots, certain deviations can be seen where model test maximum force decrease with increased free span height and design load maximum force increase with increasing free span height. The 350 mm pipeline case is an exception, it increases from 0.25 m to 0.5 m free span and then decreases with 0.75 m free span. In the fixed case, a possible trend can be observed where the maximum pull over force increase with increasing free span.

In general, the results are somewhat similar as they range from approximately 0.6 to 1.0 in all cases, making it difficult to conclude with a clear trend including all cases. It should be considered that some of this differences can be attributed to coincidences, where small variations in the simulations or model tests can lead to severe alterations in results.

The effect of increased span height is greatest for small diameter pipe lines, and decreases with increased pipe diameter.

5.2.4 Effect of added mass variations

An added mass test was performed to see if added mass variations were significant for pull over results. It was important to check if the choice of added mass coefficient equal to 1.0 was acceptable or if it should be altered. One hypothesis was that pipeline mass and clump weight mass would be very large compared to added mass, hence making the result more or less independent of added mass and added mass factor.

A factor of 2.29 and a reduction factor of 0.8 to account for finite cylinder length is recommended when calculating added mass for a clump weight [5]. This results in a factor of 1.832. However, at impact the clump weight will be lifted over the sea bed, and a factor of 1.3 could be used [6]. It is possible to argue that during pull over, the clump weight will be a part of the pipeline and thus free spanning. According to a recommended practice for free spanning pipelines, DNV-RP-F105, a factor of approximately 1.0 is recommended [4]. Results from simulations with different added mass coefficients is shown in figure 5.20 for 840 mm diameter pipeline, and in figure 5.21 for 350 mm diameter pipeline. The largest variance is found for the 840 mm diameter case.

The results indicate that pull over force time histories are not influenced by change in added mass.

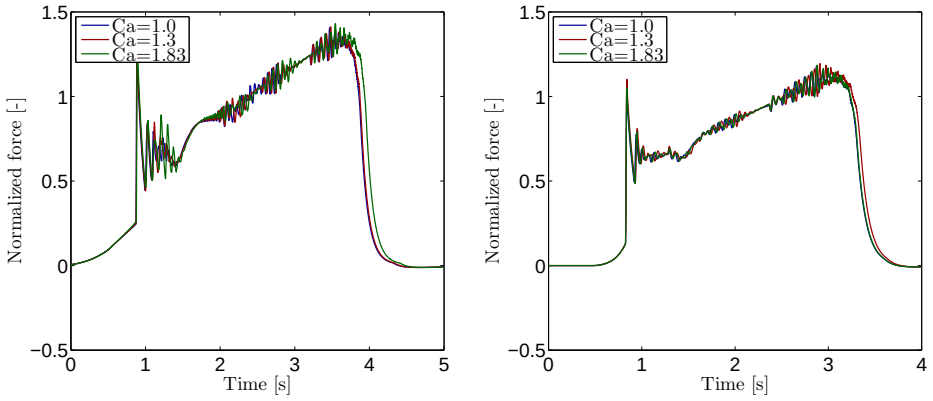

(a) 0.75 m free span height (b) 0.25 m free span height

Figure 5.20: Pull over force dependence with added mass variations, 840 mm pipeline, flexible condition

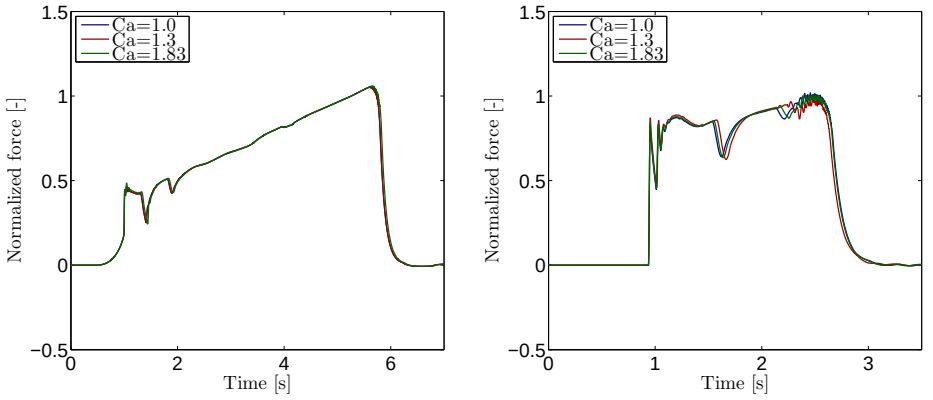

(a) 0.75 m free span height (b) 0.25 m free span height

Figure 5.21: Pull over force dependence with added mass variations, 350 mm pipeline, flexible condition

5.2.5 Effect of warp line bracket geometry

One challenge in this master thesis has been to reduce the pull over force as a mean to be similar to the corresponding model test results, especially for larger diameter cases. A change in warp line bracket geometry was attempted. This was done after measuring the clump weight design drawing in appendix A, finding the warp line bracket to be 1 mm longer than earlier

measured. 1 mm correspond to 4 cm in full scale. This change reduced the pull over force and time noticeably. Figure 5.22 show maximum pull over normalized force and corresponding time for 0.75 m free span, flexible condition, for all three diameters. In the figure, "short" describes the original warp line bracket length, and "long" describes the 4 cm elongated bracket.

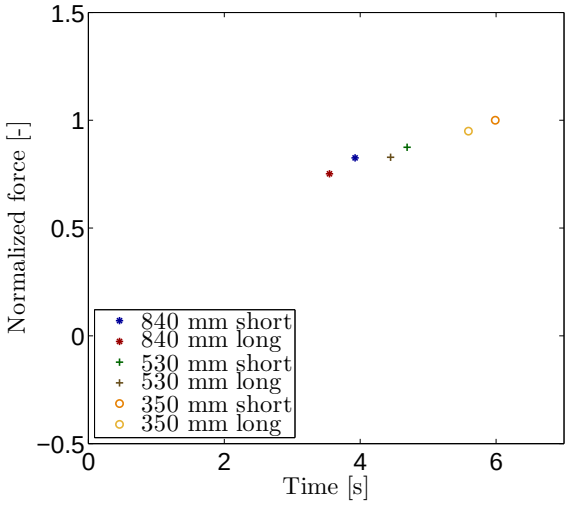

Figure 5.22: Pull over force dependence on warp line bracket geometry, 0.75 m free span height

Transients were reduced with a longer warp line bracket. This could be due to a larger contact area between warp line bracket and pipeline. With a larger contact area a reduction in high frequency clump weight pipeline shock will occur, and it will be easier for the clump weight to slide over the pipeline.

Trawl equipment, including clump weight, vary between the different trawl boats. Therefore it is interesting to see what a small change in clump weight geometry can lead to, when considering clump weight pipeline pull over force. This sensitivity demonstrate that a small change in clump weight design could have a noticeable effect on the pull over force, and this knowledge should be incorporated in future clump weight designs.

The effect of centre of gravity in clump weight was investigated by Kristian Maalø in his master thesis, where 10% and 20% of the clump weight mass was moved to the front beam. His main finding was that with a forward clump weight centre of gravity, pull over loads were reduced [12]. This is

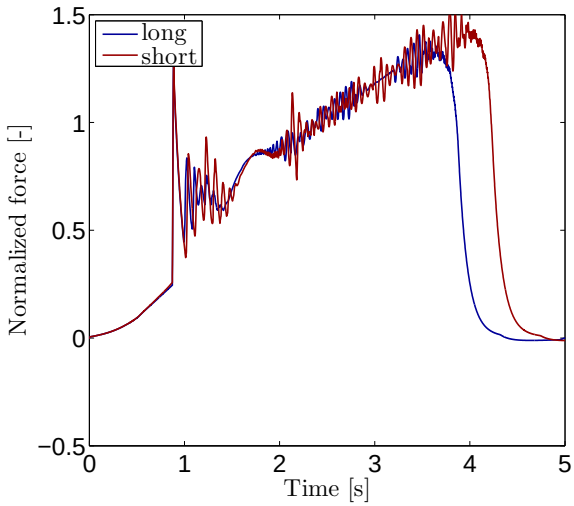

Figure 5.23: Pull over force dependence on warp line bracket geometry showing change i transients, 840 mm, 0.75 m free span height

not investigated further in this master thesis.

5.2.6 Effect of an uneven seabed

At the time of research, only a flat seabed along the clump weight path has been simulated. As earlier analyses have shown, small changes in model configuration and in clump weight angle of attack can result in significant effects regarding results. For this reason, it would be interesting to see what effect a small bump in the clump weight seabed path would have on results, as this is believed to interfere with the clump weight impact progress.

The bump was modelled to be 10 cm high and 20 cm wide. An attempt of making the bump only 10 cm was performed, but even though it showed on pull over results it was difficult to notice any changes when looking at the simulation in Xpost regarding time step seize. As results from 20 cm and 10 cm width bumps were alike, it was natural to continue with the configuration which was visible when running Xpost, hence a width of 20 cm was utilized.

Several uneven seabed sensitivities were simulated, where the distance between bump and pipeline were altered. The distance is measured from end of bump to start of pipeline. Sensitivities were performed for 840 mm

and 350 mm flexible pipelines, both with 075 m free span and 0.25 m free span, to see if there were variations between free span heights and pipeline diameters.

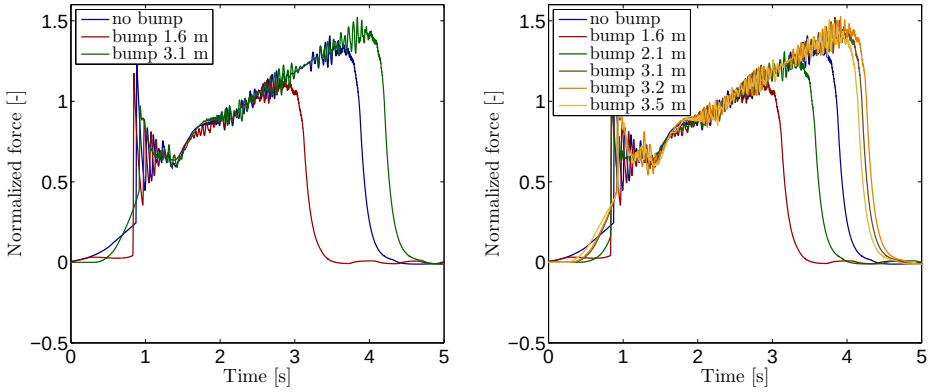

(a) Effect of uneven seabed (b) Effect of uneven seabed, more variations

Figure 5.24: Effect of uneven seabed, 840 mm, 0.75 m free span flexible condition

Figure 5.24 show the same sensitivity in both a) and b), but b) has more alterations of bump-distances included. The pull over force seemed to decrease with decreasing distance. This holds true until a threshold limit where the warp line already has started to lift the clump weight before or during clump weight bump interaction. Then the effect of the bump vanish. A distance of 1.6 m, when running the simulation in Xpost, is close to this limit.

For simulations with a longer distance between bump and pipeline, pull over forces gradually increases until being higher than the pull over force from a flat seabed. However, longer distances also seem to reach a threshold. The threshold is reached when the bump is so far away from the pipeline that it will land and settle on the flat seabed before impact. From figure 5.24 b) this threshold is seen where the pull over force reach a maximum for the 3.2 m case but decrease for the 3.5 m case. When running the 3.5 m case in Xpost, the clump weight is just touching the seabed before pipeline impact. This is shown in figure 5.25. Screen shots from the case with 3.2 m distance is also included and is shown in figure 5.26.

Similar results were obtained for the 840 mm, 0.25 m free span case, see figure 5.27.

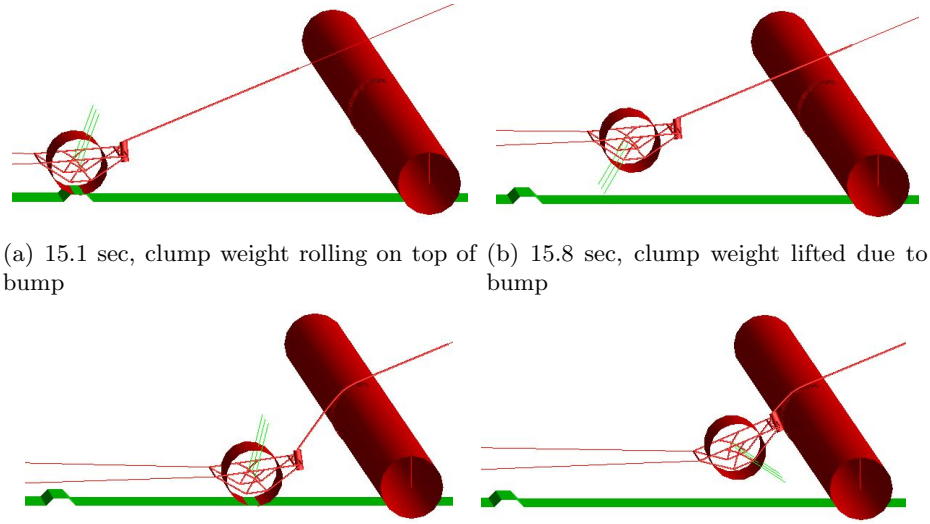

(a) 15.1 sec, clump weight rolling on top of bump

(b) 15.8 sec, clump weight lifted due to bump

(c) 16.4 sec, touching seabed

(d) 16.8 sec, at impact

Figure 5.25: Screen shots from Xpost, 0.75 m free span, 840 mm flexible condition, bump distance 3.5 m

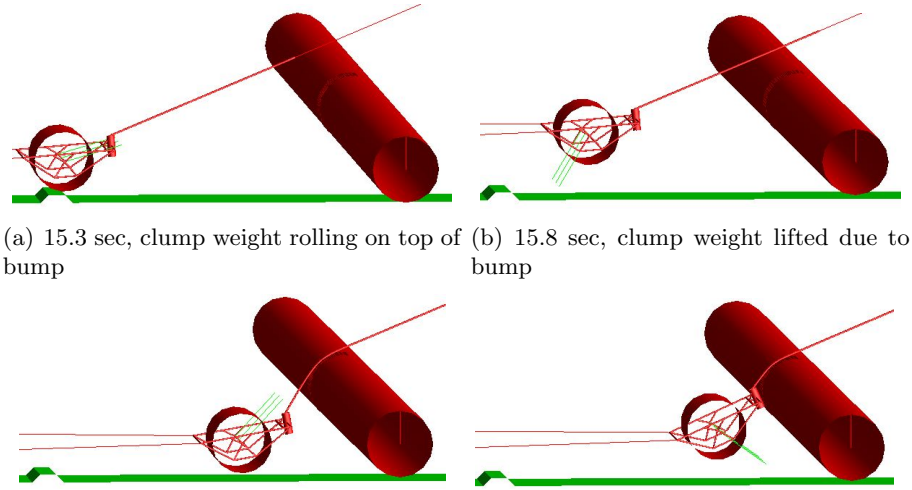

(a) 15.3 sec, clump weight rolling on top of bump

(b) 15.8 sec, clump weight lifted due to bump

(c) 16.5 sec, clump weight not touching seabed

(d) 16.8 sec, at impact

Figure 5.26: Screen shots from Xpost, 0.75 m free span, 840 mm flexible condition, bump distance 3.2 m

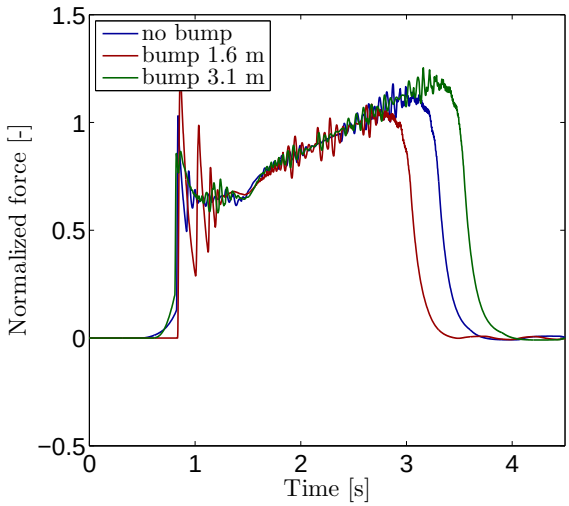

Figure 5.27: Effect of uneven seabed, 840 mm, 0.25 m free span flexible condition

For the 350 mm 0.75 m free span case (figure 5.28) same tendencies are observed. However, the bump distance in the far away case is slightly altered to make sure the clump weight is not touching the seabed after bump. A sensitivity of 350 mm, 0.25 m seabed was also attempted. In the 0.25 m case it could seem like the bump had a small range where it affected the results, as the pipeline is close to the seabed and having a small diameter.

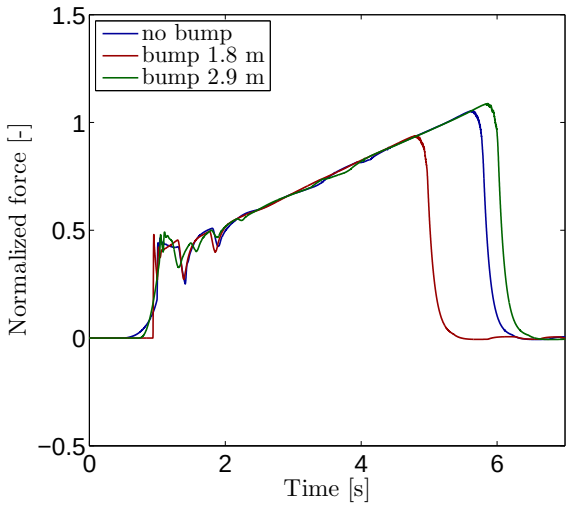

Figure 5.28: Effect of uneven seabed, 350 mm, 0.75 m free span flexible condition

5.2.7 Effect of variation in warp line angle

All analyses were simulated with a warp line angle of 23°, but during towing it is difficult to keep this angle constant at all times. Therefore, a sensitivity study altering the warp line angle was performed. The warp line angle was increased and then decreased with 20% of original value. The length of warp line was also altered as the water depth was kept constant. Ensuring sensitivities only depending on warp line angle, the axial stiffness of the warp was altered for the various lengths, maintaining a constant warp stiffness for all simulations. A summary of warp line angle, length and axial stiffness is shown in table 5.3, and screen shots from Xpost with three different warp angles is shown in figure 5.29.

Warp line angle	**Length of warp line [m]**	**Axial stiffness [N]**
23°	894	$2.685 * 10^7$
18.4°	1101	$3.304 * 10^7$
27.6°	750	$2.25 * 10^7$

Table 5.3: Summary of warp line angle, length and stiffness

This sensitivity study was performed for four different pipeline configurations. Results are shown in figure 5.30, 5.31, 5.32 and 5.33. Two

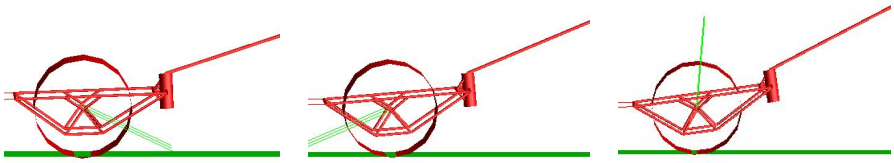

(a) Warp angle 18.4° (b) Warp angle 23° (c) Warp angle 27.6°

Figure 5.29: Screen shots from Xpost showing warp angle variations

sub figures are included in each case, where one is tuned to demonstrate differences having the same impact time, and the other illustrate how the different cases differ at time of impact. All figures indicate that a reduction in warp line angle lead to a higher pull over force, while an increase in warp line angle leads to a reduced pull over force.

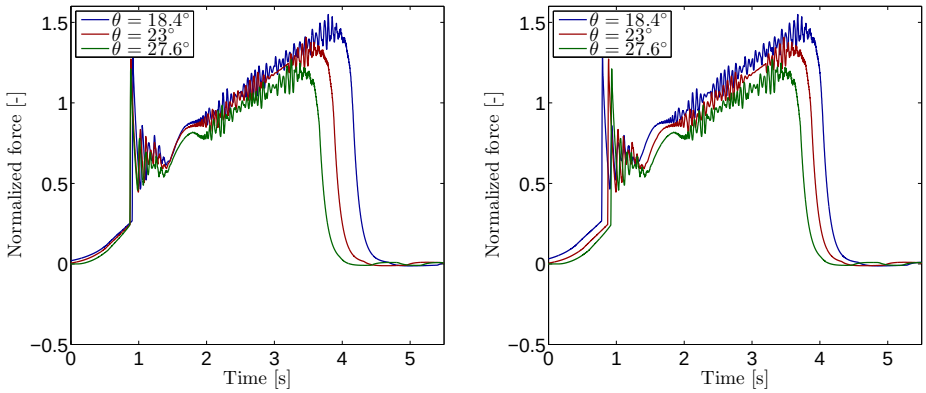

(a) Pull over force with same impact time (b) Real pull over time-force relation

Figure 5.30: Pull over force dependence on warp line angle, 840 mm, 0.75 m free span, flexible condition

According to DNV-RP-F111, a typical warp line length is between 2.5 to 3.5 times the water depth [5]. As the water depth is 350 m in these simulations, a warp line length between 875 m and 1225 m is normal. Thus, an increase of pull over force due to decreased warp line angle is not unreasonable.

When changing warp line lengths, the trawler will not necessarily change the warp line, and thereby leave the cross sectional area and modulus of elasticity unaltered. Thus, the same simulated models were executed without altering of axial stiffness as well. Pull over results were closely

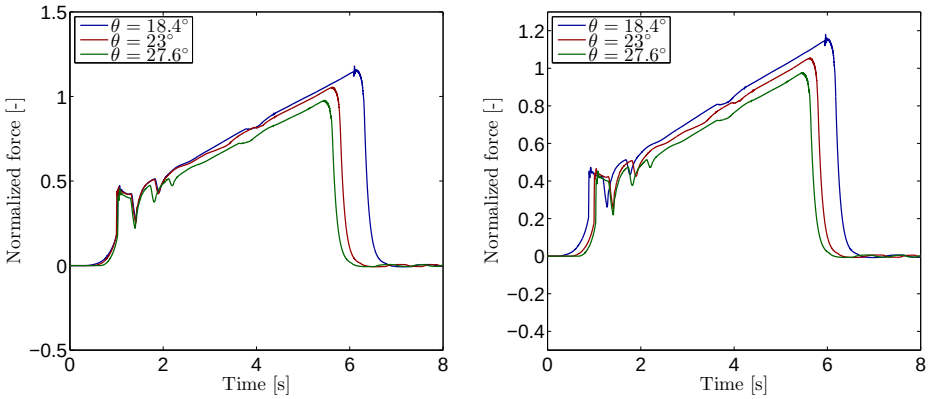

(a) Pull over force with same impact time (b) Real pull over time-force relation

Figure 5.31: Pull over force dependence on warp line angle, 350 mm, 0.75 m free span, flexible condition

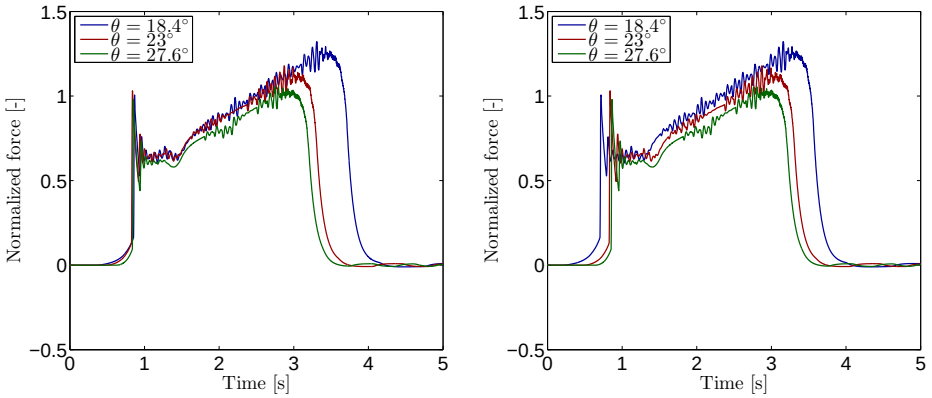

(a) Pull over force with same impact time (b) Real pull over time-force relation

Figure 5.32: Pull over force dependence on warp line angle, 840 mm, 0.25 m free span, flexible condition

related to pull over results from the constant warp stiffness cases. Thus, only one case without axial stiffness alteration is included and is shown in figure 5.34.

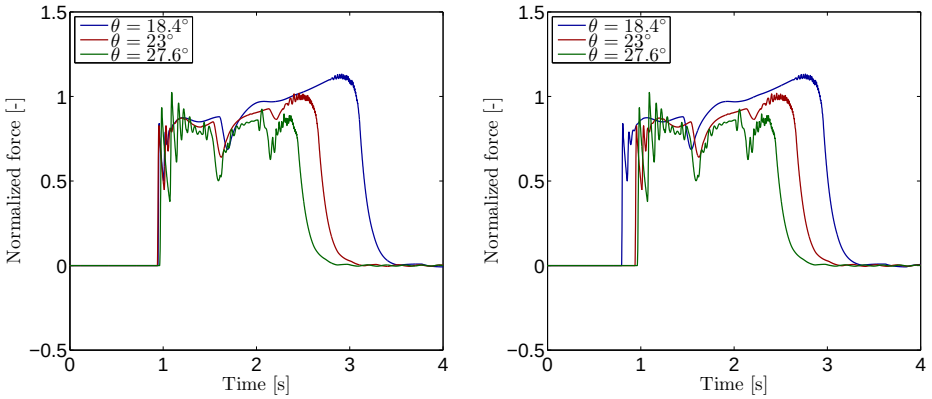

(a) Pull over force with same impact time (b) Real pull over time-force relation

Figure 5.33: Pull over force dependence on warp line angle, 350 mm, 0.25 m free span, flexible condition

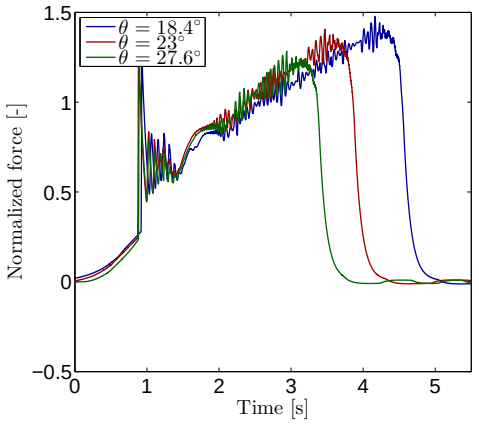

Figure 5.34: Pull over force dependence on warp line angle, 840 mm, 0.75 m free span, flexible condition, not altered axial stiffness in warp

5.3 Full scale pipeline model

A full scale pipeline model was introduced to see whether a detailed model is necessary when analysing clump weight pipeline interaction. Simulations were compared to design loads calculated from DNV-RP-F111 in flexible condition.

5.3.1 Full scale pipeline 350 mm pipe diameter

Results from 350 mm simulations were as expected, where design loads are considerably higher and have longer pull over time than the corresponding simulation result. The pull over force increase with increasing free span heigh for both design load and simulating force.

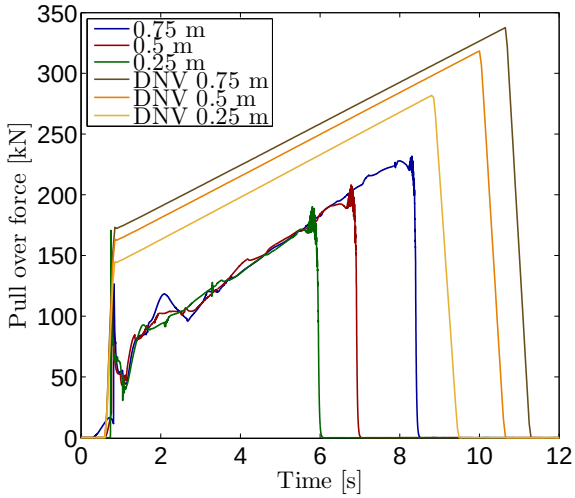

Figure 5.35: Full scale pipeline model: 350 mm diameter

5.3.2 Full scale pipeline 530 mm pipe diameter

Results from 530 mm full scale free spanning simulations is shown in figure 5.36.

Here, a deviation from the standard development is evident. The 0.75 m free span simulation case has shorter pull over time than the 0.5 m free span case, while the pull over forces are similar. When comparing these simulations in Xpost, it is difficult to see a distinct disparity between the 0.75 m and 0.5 m case, except that the 0.75 m free span case has a shorter pull over time by approximately 0.5 seconds. But according to the pull over results from these two simulations, the 0.75 m case appear to be hitting the pipeline in such a way that the clump weight is more easily pulled over the pipeline. As the distinctions between the two free span models are minor, one explanation might be that an irregularity occurs just before clump weight pipeline impact, as the warp line is pulling the pipeline slightly

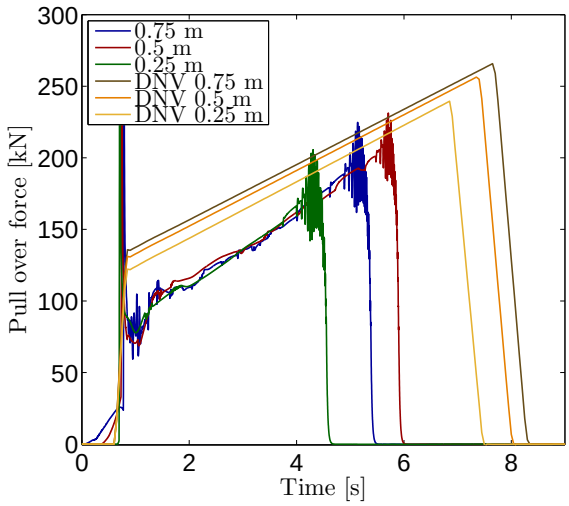

Figure 5.36: Full scale pipeline model: 530 mm diameter

downward. The warp line will pull the pipeline downward in all simulations, including the 0.5 m and 0.75 m free span case. Due to warp line pulling, an initiation of small pipeline oscillations could occur, not possible to verify visually with the time step size used. Regarding oscillations, a very small phase difference could appear just before clump weight pipeline impact, influencing where and when the clump weight actually hits the pipeline. This phase difference could be different for the two cases resulting in different time histories. The dissimilarities could also be a consequence of differences in warp line angle at time of impact, as the warp line will act differently with a deflected flexible pipeline than in the rigid pipeline cases.

5.3.3 Summary full scale free spanning pipeline results

A summary of full scale free spanning pipeline results is shown in figure 5.37.

Figure 5.37 show that design loads match simulation forces more closely for larger diameter pipelines. For the 350 mm pipeline diameter there is a larger gap between the design load and simulation force with the design load being noticeably higher.

When comparing figure 5.35 with figure5.36, two main findings are apparent. The 350 mm cases have a longer pull over time than the 530 mm cases, but

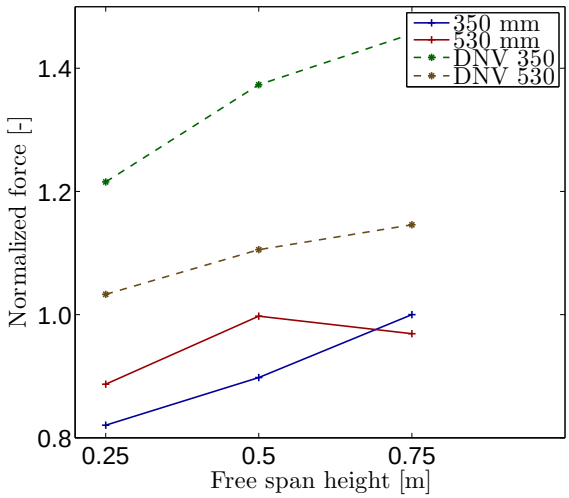

Figure 5.37: Full scale pipeline maximum pull over force

also a lower pull over force. Earlier, findings from rigid pipelines indicated a relation between pull over force and time, where the pull over force increased with increasing pull over time. Here, the analysed pipelines have correct material properties with longer free span width and reduced lateral free span stiffness. The 530 mm case have a higher deflection resistance than the 350 mm case, due to a higher mass and a higher bending stiffness in the pipeline. The high deflection resistance could lead to an event where the clump weight is more easily pulled over the pipeline, resulting in a shorter pull over time than in the 350 mm case. However, with a lower deflection resistance, the pipeline will to a larger extent be deflected horizontally by the clump weight and warp line. Thus, increasing pull over time and reducing inertial forces when clump weight is pulled over the pipeline, resulting in a lower pull over force in the 350 mm case. This effect is documented in an OMAE paper from 2012 as well [10].

Design loads are much higher than the corresponding simulated pull over force in all occurrences, which reflects a high safety factor included in the design load calculations. The design loads have a linear force time progress, while simulated results are calculated with a non-linear impact progress having geometrical non-linearities due to deformations in the pipe and a non-linear stiffness construction. This might play a role in the difference in pull over histories. More importantly, the two simulated diameter cases show an indication of pull over force reduction with decreasing pipeline stiffness, i.e with decreasing pipeline diameter, when full scale pipeline

analyses are performed. The effect of pipe stiffness is not included in the design load, and leads to a larger gap between design load and full scale pipeline pull over forces with small diameters having a lower pipeline stiffness.

A summary of maximum pull over force percentage deviation from design loads can be seen in table 5.4.

		350 mm		**530 mm**	
		SIMLA	DNV	SIMLA	DNV
		[%]		[%]	
Flexible	0.75 m	-45,6	0,0	-18,3	0,0
	0.5 m	-53,0	0,0	-10,9	0,0
	0.25 m	-48,1	0,0	-16,4	0,0

Table 5.4: Percentage deviation between simulation maximum pull over force and design load, full scale model

5.3.4 Importance of varied parameters in the clump weight pipeline analyses

A table differentiating between which sensitivity parameters assumed to be important for pull over analyses can be seen in table 5.5.

	Unimportant	Possibly important	Important
Pipe diameter			X
Free span height			X
Pipeline interaction (flexibility)			X
Warp line angle		X	
Warp line bracket geometry		X	
Wobbling		X	
Added mass	X		
Uneaven seabed (bump)		X	

Table 5.5: Parametric effect on force interaction during pull over analyses

Chapter 6

Conclusion

The main objective when analysing experimental test models is to obtain a resilient numerical model with similar pull over force-time histories as found in the model test. When comparing the experimental test model simulation results in the master thesis with corresponding model test cases, an apparent conformity is established in most cases. However, 0.25 m free span cases emerge with certain deviations, especially in fixed condition. The largest deviation is found for 530 mm 0.25 m fixed case, which deviate -39.7% from the corresponding maximum model test pull over force. The gap between model test and simulated results could be caused by a lack of friction in simulation analyses. Friction could be more important for low free spans related to direct clump weight pipeline interaction without having a major influence of the warp line, hence making the gap larger in the low free span cases. Further research is required to reduce this gap, and could be caused by other factors as well, e.g hydrodynamical effects. The smallest deviation when comparing results visually including pull over time are the 350 mm and 530 mm 0.5 m free span fixed conditions, having deviations of 1.2% and 6.3% respectively.

Design loads are generally higher than corresponding model test results. Exceptions are found for the 840 mm and 530 mm fixed design loads, where the deviations are -36.8% and -11.8% respectively. When comparing the design load with pull over force from experimental test model simulations, a shift is experienced where the design load has a steeper increase in pull over force, than the simulation force for decreased pipe diameter.

Several sensitivities and experimental test model simulations have shown

that the free span height and pipeline diameter is important for results. The clump weight angle of attack is influenced by diameter size and free span height. A small inclined angle of attack has shown to result in a lower pull over force, while a larger inclined angle results in a higher pull over force. With a low free span, the diameter size is the most important parameter, as the clump weight angle of attack will be relatively alike for all three diameter pipelines. Thus, for a free span height of 0.25 m, the highest pull over force is obtained for the largest diameter pipeline, where the clump weight pull over distance is the longest. For higher free spans, the clump weight angle of attack is more varied among the different pipeline diameters. The clump weight will hit the pipeline in a more inclined way for small diameter pipelines, resulting in a higher pull over force for small diameter pipelines having high free spans.

For the 350 mm simulations, results show a significant difference between the simulated rigid experimental test model and the simulated full scale model. For the full scale model, the pipeline is deflected and relocated with the clump weight pulling, allowing the clump weight longer time before being pulled over. This leads to reduced inertial forces to pull the clump weight over the pipeline, reducing the pull over force. The full scale model has a significantly lower pull over force and longer pull over time, than the corresponding experimental test model. This effect decrease when pipeline diameter is increased, since the stiffness in the pipe increases.

Pull over results from the full scale model compared to design loads show a major gap in results, where design loads have significantly higher pull over force and longer pull over time. The gap is increasing with decreasing pipeline diameter. The gap increase is likely a consequence of simplification of the design load calculations, disregarding pipeline interaction flexibility. Full scale pipeline simulations indicate that pipeline interaction flexibility has a major effect on pull over forces for low pipeline diameters.

A sensitivity analysis examining clump weight wobbling was performed, after a video of a model test showed wobbling for a test case with an irregular low pull over force. Several simulations with varied wobbling were analysed. Increased wobbling reduced the simulation pull over force by 20%, down to the initial model test pull over force value. Here, the main finding was that pull over forces will most probably be reduced if clump weight wobbling is present.

An attempt to alter warp line bracket geometry was also performed. This was based on a reassessment of design drawings for the clump weight, and

resulted in an elongation of the warp line bracket with 4 cm. As the contact area between clump weight and pipeline increased, the warp line bracket was able to glide over the pipeline more easily, reducing high shock motions and resulting in lower pull over force and time. In the 840 mm 0.75 m flexible case, an increase of warp line bracket length with 4 cm resulted in a decrease of pull over force with 10%. It should be noticed that a change in clump weight geometry influence the pull over force, and should be taken into consideration in future clump weight designs.

An analysis to see what a warp line angle alteration could lead to, in relation to pull over force was executed. The warp line angle was increased and then decreased with 20% from the original value. Results showed that a reduction of warp line angle by 20%, led to an increase in pull over force and time by approximately 10%, while an increase in warp line angle by 20%, lead to an reduction in pull over force and time by approximately 10%.

As several sensitivity analysis results indicate that small changes in model configuration could affect pull over results, simulations examining sea bed bump effect was performed. The bump had a fixed size, but the pipeline bump distance was varied. Results demonstrate that a bump in the seabed can both cause a reduction and an increase in the pull over force. The result of each distance depend on free span height and pipe diameter. When the clump weight touched the sea bed before interacting with the pipeline, the result matched a flat sea bed simulation. A shorter bump pipeline distance resulted in lower pull over force, as the clump weight in this scenario will hit the pipeline in the same way as in a low free span height. However, with a longer distance between bump and pipeline, the clump weight is angled, making the clump weight impact angle steeper, resulting in a higher pull over force.

Further research

While many of the simulated model test cases resemble results from the experimental model test, there are still some cases where the discrepancies between pull over time histories are too big. One way of trying to reduce discrepancies could be to introduce friction in the simulations.

Further research of free span and diameter alteration impact on pull over forces could be performed. A reliable limit for pipeline diameter influence on pull over force, regarding the free span height, could be established by performing more analyses where these parameters are altered.

An in-depth study of the full scale model could be performed, exploring the effects of pipe material properties with pipeline diameter change related to pull over results. This can be further employed if recommended practise for design load calculation is updated. In that regard, also more experimental test model simulations should be performed, varying the parameters identified as important.

Changes in clump weight geometry and mass could also be utilized to obtain more and varied analysis data on clump weight pipeline interaction. The data could could be further employed in new clump weight designs.

Bibliography

[1] Petroliumskartet, oljemuseet, 2005.

[2] Y. Bai and Q. Bai. *Subsea pipelines and risers*. Elsevier, 2005.

[3] Robert D. Cook, David S. Malkus, Michael E. Plesha, and Robert J. Witt. *Consepts and applications of finite element analysis*. John Wiley and Sons, INC, 4th edition, 2012.

[4] DNV, Høvik, Norway. *Recommended practice DNV-RP-F105, Free spanning pipelines*, 2006.

[5] DNV, Høvik, Norway. *Recommended practice DNV-RP-F111, interference between trawl gear and pipelines*, 2010.

[6] O. M. Faltinsen. *Sea loads on ships and offshore structures*. Cambridge University Press, 1990.

[7] Ragnar Sigbjørnsson Ivar Langen. *Dynamisk analyse av konstruksjoner*. Tapir, 1979.

[8] Ludvig Karlsen. *Redskapsteknologi i fiske*. Universitetsforlaget, 1989.

[9] Ludvig Karlsen. *Redskapslære og fangstteknologi*. Landbruksforlaget, 1997.

[10] Hagbart Alsos Kristian Maaløe, Svein Sævik. Detailed analysis of clump weight interference with subsea pipelines. In *OMAE2012*, OMAE2012-83869. ASME, 2012.

[11] Vegard Longva. Simulation of trawl loads on subsea pipelines. Master's thesis, NTNU, Department of Marine Technology, 2010.

[12] Kristian Maaløe. Clump weight trawl gear interaction with submarine pipelines. Master's thesis, NTNU, Department of Marine Technology, 2011.

[13] Kjell Magne Mathisen. *Large displacement analysis of flexible and rigid systems considering displacement-dependent loads and nonlinear constraints*. PhD thesis, NTNU, Department of Structural Engineering, 1990.

[14] Martin Troels Møller. Simulation of interference between trawl gear and pipelines. Master's thesis, NTNU, Department of Structural Engineering, 2009.

[15] Torgeir Moan and Svein Sævik. Lecture notes in tmr4505-advanced structural analysis. NTNU, Department of Marine Technology, 2011.

[16] Ivar Nygaard. Kristin and snøhvit pipelines in free spans, overtrawling by clump weights, model tests. Technical Report 580005, MARINTEK, 2004.

[17] Richard Verley Olav Fyrileiv, Dag Ø. Askheim and Hanne Rolsdorph. Pipeline trawl interaction: Effect of trawl clump weights. In *OMAE2006*, OMAE2006-92128, 2006.

[18] Niels Ottosen and Hans Petersson. *Introduction to the finite element method*. Prentice Hall, 1992.

[19] Gro S. Baarholm Svein Sævik, Ole D. Økland and Janne K. Ø. Gjøsteen. *SIMLA User manual*. MARINTEK, 3.16 edition, 2012.

[20] Svein Sævik. *SIMLA- Theory manual*. MARINTEK, 2008.

[21] Erik Levold Håvar Ilstad Per Teigen Vegard Longva, Svein Sævik. Dynamic simulation of free spanning pipeline trawl board pull over. In *OMAE2011*, OMAE2011-49592. ASME, 2011.

Appendix A

Thyobrøn roller clump weight

This appendix include a design drawing of a Thyobrøn roller type clump weight, provided to the master thesis of Kristian Maalø, from the manufacturer [12]. Cross sectional properties used in simulations during this master thesis are initially fetched from this drawing. The drawing is from a larger clump weight than modelled, but according to the manufacturer cross sectional properties are generally not changed for the different sizes. Hence, only the roller length and wall thickness are altered from this design drawing in the simulated models.

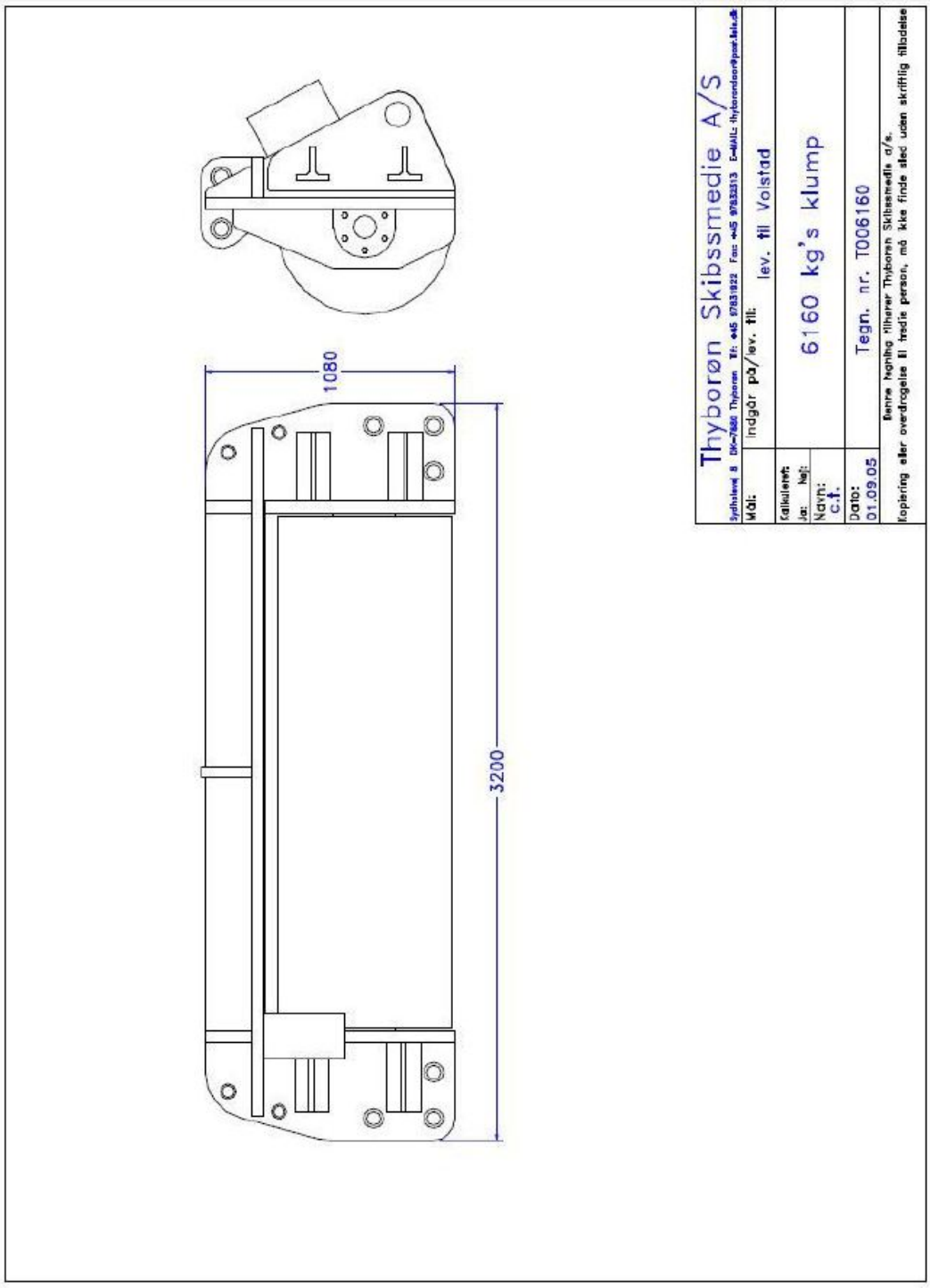
Thyborøn Skibssmedie A/S
Sydhavnen 8 DK-7680 Thyborøn Tlf: +45 97531922 Fax: +45 97532313 E-MAIL: thybornsmed@post.tele.dk
Vedr.: indgår på/lev. til:
lev. til Volstad
Kalkulerer:
Jan Højt
Navn: c.t.
6160 kg's klump
Dato: 01.09.05
Tegn. nr. T006160
Denne tegning tilhører Thyborøn Skibssmedie a/s.
Kopiering eller overdragelse til tredie person, må ikke finde sted uden skriftlig tilladelse
1080
3200

Appendix B

Additional Thyobrøn clump weight data

Clump weight properties from the drawing in appendix A, initially provided by SINTEF Fisheries and Aquaqulture, Hirtshals, Denmark, is listed below. In this master thesis, these values are provided from Kristian Maalø [12].

Description	**Symbol**	**Value**	**Unit**
Total length	l_t	2.67	m
Roller diameter	D_r	0.76	m
Roller length	l_r	1.55	m
Total dry weight	m_t	3840	kg
Ballast weights	m_b	1000	kg
Weight of frame	m_f	1400	kg
Weight of roller	m_r	1420	kg

Appendix C

Summary of normalization forces

All values compared with model test results are normalized due to restrictions in model test values. In this appendix a summary of the normalized forces are given.

Figure	Normalized on maximum pull over force from	Value [kN]
5.1 a)	Model test 3340, 840 mm 0.75 m free span flexible condition	restricted [16]
5.1 b)	Model test 3360, 840 mm 0.75 m free span fixed condition	restricted [16]
5.2 a)	Model test 3250, 840 mm 0.5 m free span flexible condition	restricted [16]
5.2 b)	Model test 3270, 840 mm 0.5 m free span fixed condition	restricted [16]
5.3 a)	Model test 3160, 840 mm 0.25 m free span flexible condition	restricted [16]
5.3 b)	Model test 3180, 840 mm 0.25 m free span fixed condition	restricted [16]
5.5 a)	Model test 3310, 530 mm 0.75 m free span flexible condition	restricted [16]
5.5 b)	Model test 3330, 530 mm 0.75 m free span fixed condition	restricted [16]
5.6 a)	Model test 3220, 530 mm 0.5 m free span flexible condition	restricted [16]
5.6 b)	Model test 3240, 530 mm 0.5 m free span fixed condition	restricted [16]
5.7 a)	Model test 3130, 530 mm 0.25 m free span flexible condition	restricted [16]
5.7 b)	Model test 3150, 530 mm 0.25 m free span fixed condition	restricted [16]
5.9 a)	Model test 3281, 350 mm 0.75 m free span flexible condition	restricted [16]
5.9 b)	Model test 3300, 350 mm 0.75 m free span fixed condition	restricted [16]
5.10 a)	Model test 3190, 350 mm 0.5 m free span flexible condition	restricted [16]
5.10 b)	Model test 3210, 350 mm 0.5 m free span fixed condition	restricted [16]
5.11 a)	Model test 3100, 350 mm 0.25 m free span flexible condition	restricted [16]
5.11 b)	Model test 3120, 350 mm 0.25 m free span fixed condition	restricted [16]
5.12	Model test 3270, 840 mm 0.5 m free span fixed condition	restricted [16]
5.13 a), b)	Model test 3340, 840 mm 0.75 m free span flexible condition	restricted [16]
5.14 a), b)	Model test 3250, 840 mm 0.5 m free span flexible condition	restricted [16]
5.17 a), b)	Model test 3160, 840 mm 0.25 m free span flexible condition	restricted [16]
5.18 a), b)	Simulated model, 350 mm 0.75 m free span flexible condition	restricted [16]
5.19 a), b)	Simulated model, 350 mm 0.75 m free span flexible condition	restricted [16]
5.20 a)	Model test 3340, 840 mm 0.75 m free span flexible condition	restricted [16]
5.20 b)	Model test 3160, 840 mm 0.25 m free span flexible condition	restricted [16]
5.21 a)	Model test 3281, 350 mm 0.75 m free span flexible condition	restricted [16]
5.21 b)	Model test 3100, 350 mm 0.25 m free span flexible condition	restricted [16]
5.22	Model test 3340, 840 mm 0.75 m free span flexible condition	restricted [16]
5.23	Model test 3340, 840 mm 0.75 m free span flexible condition	restricted [16]
5.24 a), b)	Model test 3340, 840 mm 0.75 m free span flexible condition	restricted [16]
5.27 a), b)	Model test 3160, 840 mm 0.25 m free span flexible condition	restricted [16]
5.28 a), b)	Model test 3281, 350 mm 0.75 m free span flexible condition	restricted [16]
5.30 a), b)	Model test 3340, 840 mm 0.75 m free span flexible condition	restricted [16]
5.31 a), b)	Model test 3281, 350 mm 0.75 m free span flexible condition	restricted [16]
5.32 a), b)	Model test 3160, 840 mm 0.25 m free span flexible condition	restricted [16]
5.33 a), b)	Model test 3100, 350 mm 0.25 m free span flexible condition	restricted [16]
5.34 a), b)	Model test 3340, 840 mm 0.75 m free span flexible condition	restricted [16]
5.37	Simulated free spanning model, 350 mm 0.75 m free span	231.9

Table C.1: Summary of normalization forces used in representation of results

Appendix D

Low pass filtered results

A low pass filtering of simulated results were performed to compare values from simulated results with low pass filtered values from model test results. This was executed by applying a low pass butter function in MATLAB, with threshold limit of 1.58 Hz. The low pass filter reduced the high-frequency contributions, but it did not lower the maximum pull over force. Comparison of low pass filtered results with regular non-filtered results can be seen below. Only three graphs are included, but the effect resemble in all cases.

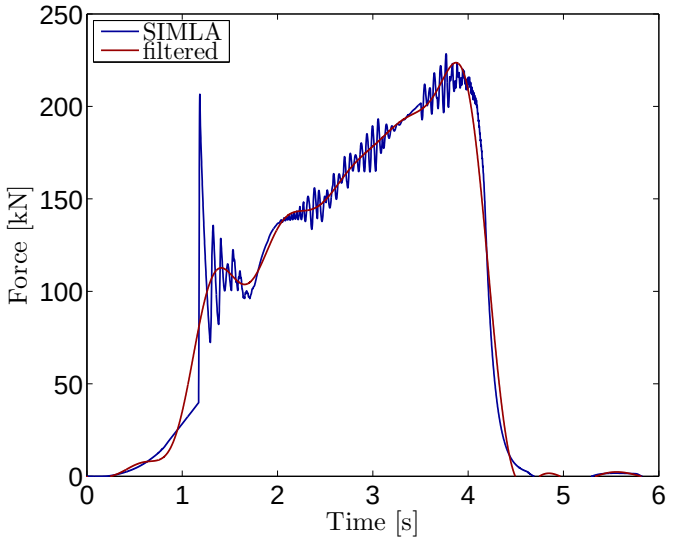

Figure D.1: Low pass filtered simulation results, filtered at 1.58 Hz, 840 mm, 0.75 m flexible condition

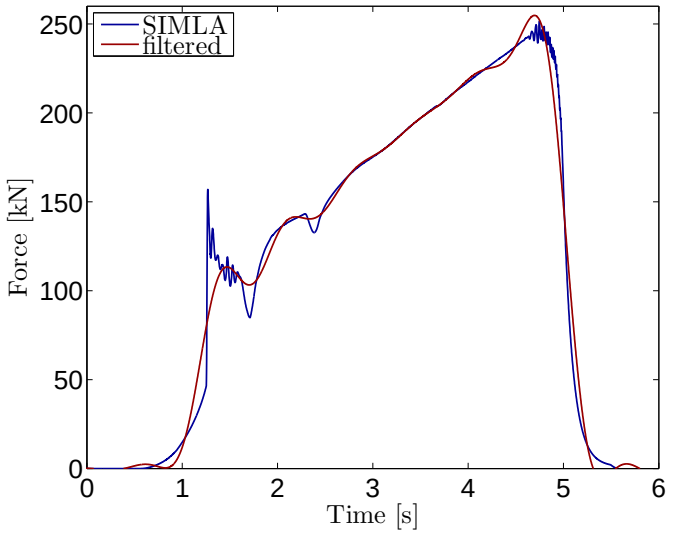

Figure D.2: Low pass filtered simulation results, filtered at 1.58 Hz, 530 mm, 0.75 m flexible condition

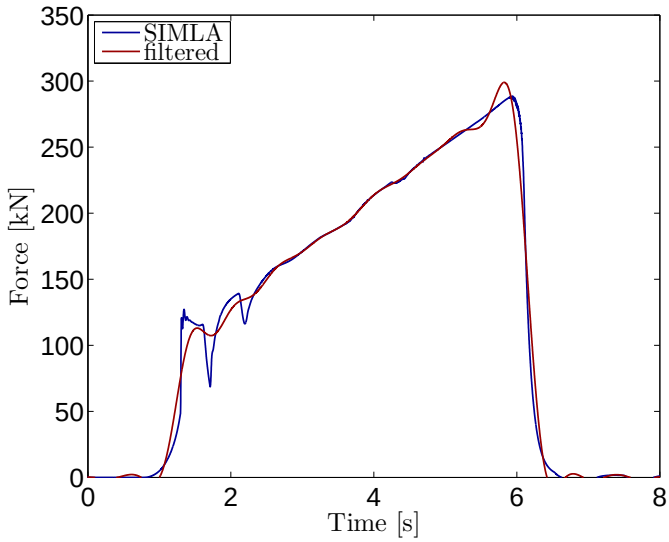

Figure D.3: Low pass filtered simulation results, filtered at 1.58 Hz, 350 mm, 0.75 m flexible condition